

https://dspace.org/

The evolution of forelimb architecture in early sauropodomorpha

Staunton, Casey Kendal

2017

https://hdl.handle.net/10539/25131

Staunton, Casey Kendal (2017) The evolution of forelimb architecture in early sauropodomorpha, University of the Witwatersrand, Johannesburg, https://hdl.handle.net/10539/25131

Downloaded from a DSpace repository. https://dspace.org/

THE EVOLUTION OF FORELIMB ARCHITECTURE IN EARLY SAUROPODOMORPHA



A Dissertation submitted to the Faculty of Science, University of the Witwatersrand, Johannesburg, in fulfilment of the requirements for the degree of

MASTER OF SCIENCE (PALAEONTOLOGY)

By Casey Kendal Staunton

Student Number: 536644

Supervisor: Prof. Jonah Choiniere

School of Geosciences and Evolutionary Studies Institute, University of the Witwatersrand, Private Bag 3, WITS 2050, Johannesburg, South Africa.











Declaration

I declare that this Dissertation is my own, unaided work. It is being submitted for the Degree of Master of Science at the University of the Witwatersrand, Johannesburg. It has not been submitted before for any degree or examination at any other University.

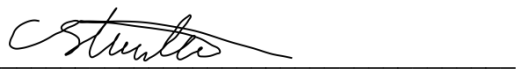

(Signature of candidate)

_____11_____day of _____August_____20_17_____in__Braamfontein

Abstract

During the evolutionary history of Sauropodomorpha, it is thought that they underwent a change from small-bodied, possibly bipedal, animals to large-bodied, quadrupedal animals. To study this transition, this thesis used photogrammetric and geometric morphometric techniques to investigate shape changes at key muscle insertion points in the humerus bone of various sauropodomorph taxa. There is noticeable shape change in the humerus from more basal to more derived Sauropodomorpha. A developmental sequence of *Massospondylus* forelimbs shows little similarity with the macroevolutionary trajectory along the sauropod stem. The former indicates that morphologies characteristic of Sauropoda began to evolve relatively early in the sauropodomorph lineage, before obligate quadrupedality appeared. The latter suggests that the quadrupedal stance of derived sauropods is not a paedomorphic retention of a juvenile state. The evolution of quadrupedality may have been a stepwise process, possibly involving some functional tradeoffs.

Acknowledgments

First to supervisor Prof. Jonah Choiniere for always being willing to answer any question, proof read any draft, and for always encouraging my passion in the field of palaeontology and sending off to various parts of the world as well as having the best open door policy.

To my wonderfully patience and supportive boyfriend Sean who has spent many hours listening to me explain this project to him and who was always willing to proof read and help me with R whenever it went wrong.

To Heinrich Mallison who was instrumental in my journey down the road of becoming a 3D modelling enthusiast. Heinrich aided me greatly in learning the ins and outs of photogrammetry and was also simply an email away no matter what the question.

To all my wonderful friends and colleagues at the ESI who are always to help, offer advice or just have a friendly chat.

To the collections managers, curators and staff of the institutions I have visited over the past two years for allowing me access to so many amazing specimens and allowing me to digitize them.

To the CoE and PAST for the funding that made this project possible

Table of Contents

Declaration _____Page i

Abstract _____ Page ii

Acknowledgments _____ Page iii

List of Figures _____ Page 1

List of Tables _____ Page 3

List of Scripts and Programs _____ Page 5

Nomenclature _____ Page 5

1.Introduction _____Page 6

2.Materials and Methods

2.1 Materials _____Page 11

2.2 Methods_____Page 14

3.Results

3.1 Proximal Set of Landmarks _____Page 36

3.2 Distal Set of Landmarks _____ Page 38

3.3 Complete Set of Landmarks _____ Page 41

3.4 Fossae Set of Landmarks _____Page 44

3.5 Proximal Ontogeny Set of Landmarks _____ Page 46

3.6 Distal Ontogeny Set of Landmarks_____ Page 48

3.7 Fossae Ontogeny Set of Landmarks _____ Page 50

4.Discussion

4.1 Morphology changes of the humerus and posture _____ Page 53

4.2 *Massospondylus* ontogeny_____ Page 61

4.3 Paedomorphosis in locomotory evolution of Sauropoda _____ Page 63

5.Conclusion _____Page 65

Appendix 1 _____Page 66

Appendix 2 _____Page 70

Appendix 3_____Page 75

Appendix 4_____Page 84

Appendix 5_____Page 86

6.References _____ Page 88

List of Figures

Figure (1): A recent phylogeny of Sauropodomorpha compiled by McPhee *et al* 2014

Figure (2): Proximal landmarks of the left humerus used in this study.

Figure (3): Distal landmarks of the left humerus used in this study.

Figure (4): Complete landmarks of the left humerus used in this study

Figure (5): Olecranon fossa and cuboid fossa landmarks of the left humerus used in this study.

Figure (6): PCA plot of PC1 vs PC2 of the proximal set of landmarks

Figure (7): PCA plot of PC1 vs PC2 of the distal set of landmarks

Figure (8): PCA plot of PC1 vs PC2 of the complete set of landmarks

Figure (9): PCA plot of PC1 vs PC2 of the olecranon and cuboid fossa of the distal humerus landmarks

Figure (10): PCA plot of PC1 vs PC2 of the proximal set of ontogeny landmarks

Figure (11): PCA plot of PC1 vs PC2 of the distal set of ontogeny landmarks

Figure (12): PCA plot of PC1 vs PC2 of the fossas set of ontogeny landmarks

Figure (A1): PCA plot of PC2 vs PC3 of the proximal set of landmarks.

Figure (A2): PCA plot of PC2 vs PC3 of the distal set of landmarks

Figure (A3): PCA plot of PC2 vs PC3 of the complete set of landmarks.

Figure (A4): PCA plot of PC2 vs PC3 of the olecranon and cuboid fossa of the distal humerus landmarks.

Figure (A5): PCA plot of PC2 vs PC3 of the proximal set of ontogeny landmarks.

Figure (A6): PCA plot of PC2 vs PC3 of the distal set of ontogeny landmarks.

Figure (A7): PCA plot of PC2 vs PC3 of the fossae set of ontogeny landmarks.

Figure (A8): Logged Centroid Size vs principal Components of interest for the proximal set of landmarks.

Figure (A9): Logged Centroid Size vs Principal Components of interest for the distal set of landmarks.

Figure (A10): Logged Centroid Size vs Principal Components of interest for the complete set of landmarks.

Figure (A11): Logged Centroid Size vs Principal Components of interest for the cuboid fossa and olecranon fossa set of landmarks.

Figure (A12): Logged Centroid Size vs Principal Components of interest for the proximal ontogeny set of landmarks.

Figure (A13): Logged Centroid Size vs Principal Components of interest for the distal ontogeny set of landmarks.

Figure (A14): Logged Centroid Size vs Principal Components of interest for the fossae ontogeny set of landmarks.

Figure (A15): PCA plot of PC1 vs PC2 of the proximal set of landmarks where all juvenile specimens were removed

Figure (A16): PCA plot of PC1 vs PC2 of the distal set of landmarks where all juvenile specimens were removed

List of Tables

Table (1): List of specimens and their repositories.

Table (2): A list of the scaling factors used.

Table (3): List of specimens that are complete or retain only a proximal end

Table (4): Landmarks used for the proximal dataset

Table (5): List of specimens that are complete or retain only a distal end

Table (6): Landmarks used for the distal dataset

Table (7): List of specimens that are complete

Table (8): Landmarks used for the complete dataset

Table (9): List of specimens that are preserve a clear olecranon and cuboid fossa

Table (10): Landmarks used for the fossa dataset

Table (11): List of *Massospondylus* specimens that are complete or retain only a proximal end

Table (12): List of *Massospondylus* specimens that are complete or retain only a distal end

Table (13): List of *Massospondylus* specimens that preserve a clear olecranon and cuboid fossa

Table (14): Final list of specimens included in the proximal set after exclusion due to missing landmarks.

Table (15): Final list of specimens included in the distal set after exclusion due to missing landmarks.

Table (16): Final list of specimens included in the complete set after exclusion due to missing landmarks.

Table (17): Measurements taken for each specimen in the set to determine relative size groups

Table (18): Measurements taken for each specimen in the set to determine relative size groups

Table (19): Measurements taken for each specimen in the set to determine relative size groups

Table (20): Results of Goodall's F-test

Table (A1): Regression data for proximal set of landmarks using centroid size vs Principal Components of interest.

Table (A2): Regression data for distal set of landmarks using centroid size vs Principal Components of interest.

Table (A3): Regression data for complete set of landmarks using centroid size vs Principal Components of interest.

Table (A4): Regression data for Fossae set of landmarks using centroid size vs Principal Components of interest.

Table (A5): Regression data for proximal ontogeny set of landmarks using centroid size vs Principal Components of interest.

Table (A6): Regression data for distal ontogeny set of landmarks using centroid size vs Principal Components of interest.

Table (A7): Regression data for fossae ontogeny set of landmarks using centroid size vs Principal Components of interest.

Table (A8): Specimens in the proximal set missing landmarks and which numbers are missing and were excluded from the set.

Table (A9): Specimens in the distal set missing landmarks and which numbers are missing were excluded from the set.

Table (A10): Specimens missing landmarks and which numbers are missing and were excluded from the set.

Table (A11): Measured angles of humeral torsion for key specimens.

List of Scripts and Programs

Agisoft Photoscan Professional Version 1.2.6 (Agisoft LLC, St. Petersburg, Russia)

Amira version 5.4.5 (FEI Visualization Sciences Group, Merignac Cedex, France)

R version 3.3.1 (R Foundation for Statistical Computing, Vienna, Austria.)

Nomenclature

The traditional, or "Romerian," anatomical and directional terms rather than their veterinarian alternatives were used (Wilson 2006).

1.Introduction

Sauropods include the largest terrestrial animals of all time (Mazzetta *et al* 2004, Benson *et al* 2014). Although derived members of the group are generally enormous, they first evolved as small, bipedal animals (Martinez and Alcober 2009) with only the derived sauropods adopting quadrupedal postures. However while the derived sauropods have been the focus of an intensive study by Sanders and colleagues over the last ten years (e.g., Sander *et al* 2011), with particular regard to how they achieved such gigantic size, the transitional features of non-sauropodan sauropodomorphs have received less focused attention (Yates 2003, Yates and Kitching 2003, Yates 2004 and McPhee *et al* 2014). In particular, the acquisition of quadrupedal postures and the implications for changes in the anatomy of the forelimb have been relatively understudied. This is surprising, as quadrupedality is one feature generally thought to facilitate gigantic body size (Carrano 2005, Wilson 2005).

Non-sauropodan sauropodomorphs are a paraphyletic assemblage of animals that form successive sister groups to Sauropoda (Yates 2003, Yates and Kitching 2003, Yates 2004, Upchurch *et al* 2007). They were the dominant high-browsing animals from the Late Triassic until the Early Jurassic at which point they were replaced by the sauropods (Barrett *et al* 2010). Non-sauropodan sauropodomorphs are most commonly found in North America, Europe, South America and southern Africa (Kitching and Raath 1984, Galton and Van Heerdan 1985, Kermack 1984, Galton 2001, Barrett 2004, Galton and Upchurch 2004, Galton *et al* 2007, Yates 2007, Barrett 2009, Mannion 2009, Sertich and Loewen 2010, Yates *et al* 2010, Apaldetti *et al* 2011, Pol *et al* 2011, Yates *et al* 2011, Marsh 2013).

South Africa's Elliot and Clarens Formations of the Eastern Cape and Free State provinces have produced many important non-sauropodan sauropodomorph fossils (Kitching and Raath 1984), including several recent finds that suggest that the palaeodiversity of these formations may still be incompletely known (McPhee *et al* 2015, Otero *et al* 2015). Elsewhere in Gondwana, South America has also produced some of the early members of Sauropodomorpha such as *Saturnalia* (Langer *et al* 1999) and *Panphagia* (Martinez and Alcober 2009). In the last decade, dedicated phylogenetic revisions and taxonomic work aimed at clarifying the validity and diagnoses of non-sauropodan sauropodomorphs has greatly improved our knowledge of the group's evolution (e.g., Upchurch *et al* 2007, Barrett *et al* 2009,Martinez and Alcober 2009, Yates *et al* 2010, McPhee *et al* 2014, de Fabrègues and Allain 2016; see Figure (1) for a full phylogeny).

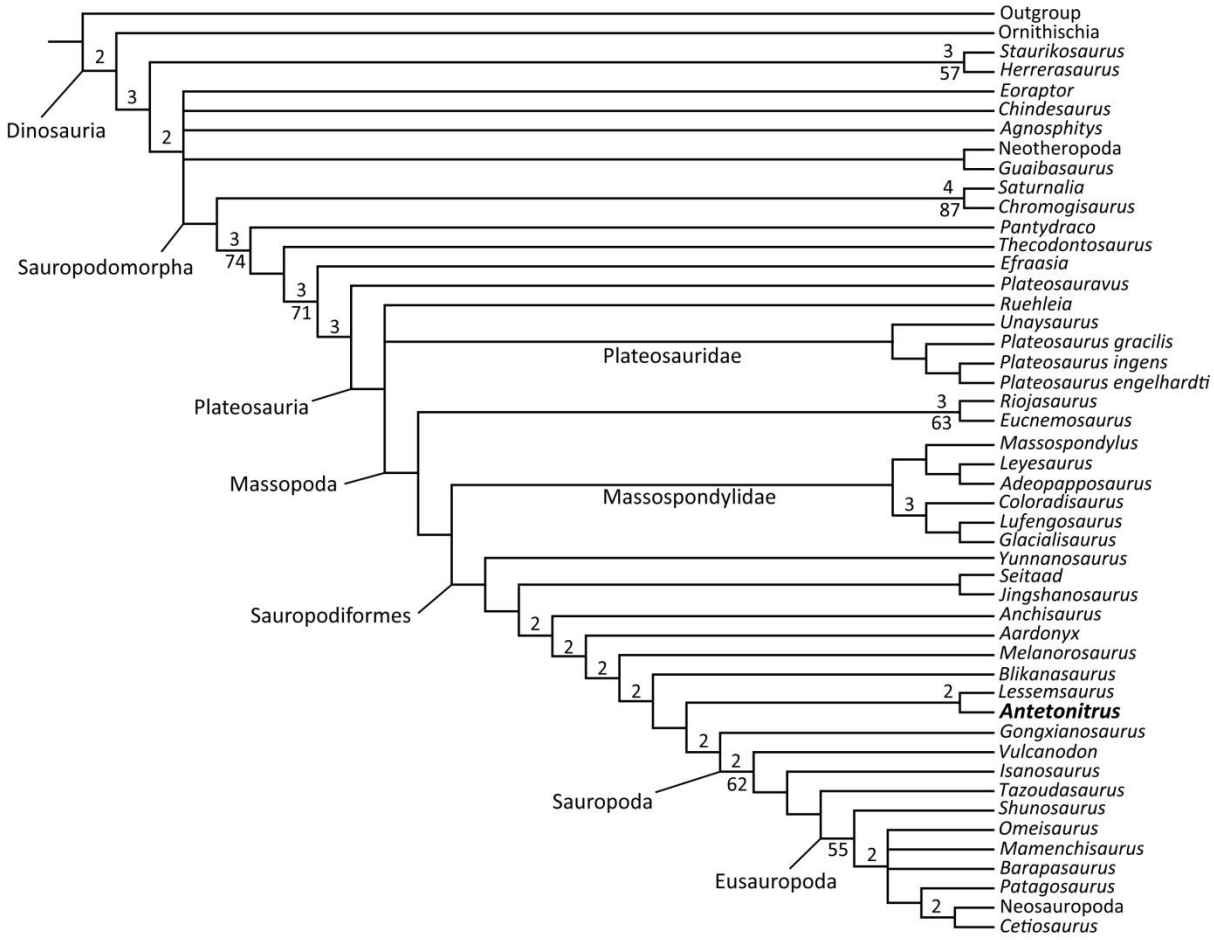

Figure (1): A recent phylogeny of Sauropodomorpha compiled by McPhee *et al* 2014

Although later sauropodomorphs are extremely large, the earliest members of the clade, such as *Eoraptor*, *Saturnalia* and *Panphagia*, were lightly built (Sereno *et al* 1993, Langer *et al* 1999, Martinez and Alcober 2009). However, analysis of the body size within the group shows that they are one of the few clades to have a strong drive trend towards an increasing body size over time (Benson *et al* 2014). This suggests that there is strong positive selection within the clade for larger body size.

Sander (2013) proposed an evolutionary cascade model for how sauropods achieved such massive size over time, hypothesizing a stepwise sequence of trait evolution where each step is a prerequisite for the next set of traits. This evolutionary cascade model may explain the strength of the trend observed by Benson and colleagues (2014), as many different factors within that model are implicated in increasing body size, such as reduced head size, long neck among others.

One thing the evolutionary cascade model was equivocal about relates to sauropods and their locomotion. Sander (2013) indicated that the graviportal stance and locomotion pattern of sauropods needs to be tested to determine whether it played a role in reinforcing gigantism. Sander (2013) then further proposed that the selective advantage from this was more energy efficient locomotion. In comparison modern mammals that attain a large body size achieve decreasing stride frequency with

increasing body size (Taylor *et al* 1982, Strang and Steudel 1990, Kilbourne and Hoffman 2013) meaning that the cost of transport would decrease with increasing size in mammals based on the amount of energy consumed per stride (Taylor *et al* 1982, Strang and Steudel 1990, Kilbourne and Hoffman 2013). In order to test such a model, particularly with regard to posture and changes in forelimb morphology, the pleisomorphic conditions for sauropodomorphs and the timing and pace of macroevolutionary events must be better understood.

Bipedalism has evolved multiple times within Archosauria, and it is the pleisomorphic condition for Dinosauria (Hutchinson 2006). Bipedal gaits in basal non-sauropodan sauropodomorphs were investigated by Remes (2008), who focused on *Saturnalia*, *Efraasia* and *Thecodontosaurus* compared to *Herrerasaurus* and *Eoraptor*. He concluded that, based on the adaptations seen, *Saturnalia*, *Efraasia*, and *Thecodontosaurus* display modifications for grasping in the forelimb, and in a quadrupedal stance these taxa would adopt a slow, semi-sprawling gait. For these reasons, Remes (2008) concluded that these animals were most likely bipedal. Langer (2003) described *Saturnalia* as a facultative biped. However later Langer et al (2007) noted several similarities between *Saturnalia* and *Herrerasaurus*, a basal dinosaur that is thought to be bipedal and close to the base of the saurchian lineage (Sereno and Novas 1992), but thought that *Saturnalia* may be quadrupedal in contrast to Remes (2008) later assessment. The fact that many of these basalmost sauropodomorphs appear to be bipedal, and that the basal most ornithischians and theropodans are bipedal, strongly indicates that this is the ancestral state for all sauropodomorphs (Wilson 2005).

Bipedalism may not, however, be the earliest ontogenetic locomotory strategy in dinosaurs. Recent work by Zhao et al (2013) on basal ceratopsians showed that *Psittacosaurus* underwent a shift in posture from quadrupedal to bipedal during its development. The authors concluded that this shift was widespread in dinosaurs including theropods (Kundrat *et al* 2008), Ornithischia (Heinrich *et al* 1993), and even in Sauropodomorpha (Reisz *et al* 2005, Reisz *et al* 2010). Therefore, in addition to studying the evolution of posture on the lineage leading to Sauropoda, changes in posture over the life span of these dinosaurs also merit consideration (Dilkes 2001, Reisz *et al* 2010, Zhao *et al* 2013).

If this ontogenetic postural shift hypothesis applies to non-sauropodan sauropodomorphs as well and all juvenile sauropods are quadrupedal, then it is worth testing if the adult derived sauropods "scale up" the quadrupedality of the babies or if they modify the limb in particular ways unique to late-stage ontogeny. However, there are contrary examples in at least some derived Ornithischians: in a study of ontogeny in hadrosaurs, Dilkes (2001) and Norman(1980) found that the hatchlings walk in a bipedal manner and become habitually quadrupedal as adults. Understanding how ontogeny affects the locomotory style has direct implications for effects on anatomy, phylogeny, and even feeding ecology. Sauropodomorphs, in particular non-sauropodan sauropodomorphs, offer an independent sample group in which to test this.

Massospondylus is the best-known non-sauropodan sauropodomorph from Gondwana. It is represented by at least 150 specimens of varying ontogenetic stages, although some taxonomic referrals are dubious. The posture of *Massospondylus* has also been a subject of much debate. *Massospondylus* has been described as a habitual quadruped that was facultatively bipedal (Bonnan and Yates 2007). However, more recent studies have indicated that *Massospondylus* is a habitual biped as an adult (Bonnan and Senter 2007). Reisz *et al* (2010), using trackways and allometric ratios in limb length data, found evidence of a postural change during ontogeny: from quadrupedal as a juvenile to bipedal as an adult. Reisz *et al* (2005) used measurements from embryos of *Massospondylus* in comparisons to the adults and found that the embryos had relatively large forelimbs, a large head, and a horizontal neck posture. This suggests that hatchlings were obligate quadrupeds while the adults were facultatively bipedal.

These ontogenetic studies have included some dedicated measures of allometry. Reisz *et al* (2005) suggests that the gait of more derived sauropods may result from postnatal negative allometry of the forelimbs. Livingston *et al (*2009) considering data from an ontogenetic series of *Alligator mississipiensis* as well as linear measurements of *Massospondylus* concluded that ontogenetic postural shifts were due to differences in growth rate of the forelimbs and hindlimbs - again alluding to negative forelimb allometry.

Even though negative forelimb allometry seems established, concomitant shape changes supporting a shift in function have not been adequately studied. To date, few studies (Yates *et al* 2010, McPhee *et al* 2014) have examined the shape changes of the forelimb during the ontogeny of non-sauropodan sauropodomorphs or across the evolutionary lineage leading to sauropods. Bonnan *et al* (2013) looked at the changing sub articular shape of the humerus and femur and articular cartilage thickness in eutherian mammals and saurischian dinosaurs. Not only did the study show that articular cartilage thickness and sub-articular shape are correlated but also showed that sub-articular shape scales differently between eutherian mammals and saurischian dinosaurs which could be the reasons behind how dinosaur reach such gigantic sizes compared to mammals. As shape changes should be strongly correlated with function, it stands to reason that they may offer a more sophisticated picture of the changing posture of these animals. This makes *Massospondylus* an ideal candidate taxon for further ontogenetic studies of the forelimb.

Sauropodomorphs show concurrent progressive morphological changes including a transition from ancestral bipedality to quadrupedality. Understanding this major locomotory transition from bipedal, relatively small bodied basal animals to massive, quadrupedal sauropods requires careful quantification of the morphology of the appendicular skeleton, particularly the forelimb. The overarching goal of this study is to understand how forelimb morphology changes on the lineage leading to Sauropoda. The humerus was selected as a proxy for the entire forelimb for several reasons:

1) it bears muscle origin and insertion points for prime drivers of forelimb motion, 2) it preserves well in the fossil record, particularly in non-sauropodan sauropodomorph fossil specimens, 3) its complex shape makes it ideal for identifying type I landmarks which allows more precise homology relationships between input data points. These more precise relationships aid in understanding the shape changes that can be related directly to muscle geometry which then in turn that affect the motion of the forelimb.

In order to evaluate how humerus shape evolves in Sauropodomorpha, and to decipher how these changes are associated with phylogeny and ontogeny, there are three main questions I tested in this thesis:

1) How does the morphology of the humerus change between non-sauropodan sauropodomorphs and more derived sauropods and what can be inferred about a possible postural shift from these changes?

2) How does the forelimb of *Massospondylus* change through an ontogenetic sequence and what can be inferred about an ontogenetic postural shift from these changes?

3) Do the changes seen in the ontogenetic sequence of *Massospondylus* resemble changes that may be seen in the sauropod lineage from more basal to relatively more derived non-sauropodan sauropodomorphs and if so are these the result of neoteny?

2.Methods-Materials

2.1 Materials

Specimens used in this analysis were selected based on availability, preservational quality, and phylogenetic position on the sauropodomorph lineage, with a goal of sampling widely across the phylogeny of the group. The complete list of specimens and their institutional repositories can be found in Table (1).

Selection criteria used to determine which specimens were included was a lack of obvious deformation and that the specimen be as complete as possible. Many specimens do not include locality data, particularly fine scale temporal data, and so this was not used in analyses.

Table (1): List of specimens and their repositories. Specimens marked with # were examined but a digital model was not produced. Specimens marked with * had a model produced via laser scanning.

Species	**Specimen Number**	**Repository**
Anchisaurus	YPM 1883	Yale Peabody Museum, New Haven, USA
Antetonitrus	BPI/1/4952	Evolutionary Studies Institute, Johannesburg, South Africa
	NMQR 1545[#]	National Museum, Bloemfontein, South Africa
Cetiosauriscus	R 3 078[#]	Museum of Natural History, London, United Kingdom
Efraasia	SMNS 12668	Stuttgart State Museum of Natural History, Germany
Massospondylus	BP/1/4934 (Big Momma)*	Evolutionary Studies Institute, Johannesburg, South Africa
	BP/1/4732*	Evolutionary Studies Institute, Johannesburg, South Africa
	BP/1/4860*	Evolutionary Studies Institute, Johannesburg, South Africa

	BP/1/4998a*	Evolutionary Studies Institute, Johannesburg, South Africa
	BP/1/4998b*	Evolutionary Studies Institute, Johannesburg, South Africa
	BP/1/4999 (proximal)*	Evolutionary Studies Institute, Johannesburg, South Africa
	BP/1/4999 (distal)*	Evolutionary Studies Institute, Johannesburg, South Africa
	BP/1/5000*	Evolutionary Studies Institute, Johannesburg, South Africa
	BP/1/5001	Evolutionary Studies Institute, Johannesburg, South Africa
	BP/1/5005*	Evolutionary Studies Institute, Johannesburg, South Africa
	BP/1/5241 (distal)*	Evolutionary Studies Institute, Johannesburg, South Africa
	BP/1/6125*	Evolutionary Studies Institute, Johannesburg, South Africa
	SAM PK 3429	South African Museum, Cape Town, South Africa
	SAM PK 5132	South African Museum, Cape Town, South Africa
Melanorosaurus	SAM PK 3450	South African Museum, Cape Town, South Africa
	SAM PK 3532	South African Museum, Cape Town, South Africa
	NMQR 1551[#]	National Museum, Bloemfontein, South Africa

Pantydraco	BMNH 19 7	Museum of Natural History, London, United Kingdom
Plateosaurus engelhardti	MBR 4430 163	Museum für Naturkunde, Berlin, Germany
	SMNS 12949	Stuttgart State Museum of Natural History, Germany
	SMNS 20664	Stuttgart State Museum of Natural History, Germany
	SMNS 53537	Stuttgart State Museum of Natural History, Germany
	SMNS 91296	Stuttgart State Museum of Natural History, Germany
	SMNS 91310	Stuttgart State Museum of Natural History, Germany
Plateosaurus gracilis	SMNS 12354	Stuttgart State Museum of Natural History, Germany
Plateosauravus	SAM PK 3342	South African Museum, Cape Town, South Africa
	SAM PK 3350	South African Museum, Cape Town, South Africa
	BPI/1/7358	Evolutionary Studies Institute, Johannesburg, South Africa
Ruehleia	MBR 4718 104 (proximal and distal)	Museum fur Naturkunde, Berlin, Germany
Sefapanosaurus	Evolutionary Studies Institute, Johannesburg, South Africa	Evolutionary Studies Institute, Johannesburg, South Africa

2.2 Methods

Photogrammetry

I used standardized photogrammetric methods to produce digital 3D models of the specimens in the analysis. Photogrammetry is a commonly used method for constructing accurate and precise digital 3D models from a set of two-dimensional photographs (e.g., Falkingham 2012, Mallison and Wings 2014). Photogrammetric methods are now commonplace in palaeontology, and have been used to: build skeletal reconstructions (Falkingham 2012, Mallison and Wings 2014); produce detailed contour maps of footprints (Breithaupt *et al* 2004, Remondino *et al* 2010, Falkingham 2012); and reconstruct full environments for taphonomic and spatial analysis purposes (Kruger *et al* 2016).

Photographic protocol

For humeral reconstructions in this project, I took a series of photographs at 45 degree increments surrounding the specimen. This photographic protocol was repeated on each humerus in lateral, medial, and anterior view. In each view a different colour material was used for background in order to reduce the effect of incorrect point matching.

Two cameras were used to take the photographs - the first was a Canon EOS 5D Mark II with a maximum resolution of 21.1 megapixels that was fitted with a Canon 100mm L-series Macro lens. The second camera used was a Canon EOS 760D with a maximum resolution of 24.2 megapixels that was fitted with a Tamron 15-30mm Wide angle lens.

Each specimen was represented by a data set consisting of jpeg images. Sets could range from between 100 to 300 images depending on the physical size of the specimen and detail require to produce a model.

Photographs were then imported into AGISoft Photoscan Pro (http://www.agisoft.com/). The following workflow parameters were used to produce the 3D models:

1. Alignment

- Accuracy: High
- Pair Selection: disabled
- Advanced settings were left as the programs original defaults

2. Dense Cloud

- Quality: High
- Depth Filtering: Aggressive

- Advanced settings were left as the programs original defaults

Spurious background information was deleted from the dense cloud at this point.

3. Mesh Generation

- Surface Type: arbitrary
- Source Data: Dense cloud
- Face Count: high
- Advanced settings were left as the programs original defaults

After mesh generation the model was exported and saved as an STL for compatibility and long-term archival purposes. All of the AGIsoft project files were also retained and saved for later use.

Some specimens were scanned in 2014 (Staunton, Honours thesis) using an Artec Eva white-light scanner with a maximum resolution of 0.5 mm. These specimens were reconstructed in Artec Studio 9 but also exported as STL files for archiving and analysis. The following specimens were produced using the Artec scanning protocol BP/1/4934, BP/1/4732, BP/1/4860, BP/1/4998a, BP/1/4998b, BP/1/4999 (proximal), BP/1/4999 (distal), BP/1/5000, BP/1/5005, BP/1/5241 (distal), BP/1/6125. They are marked in the above table with an *.

Scaling

Scaling was used to standardized to unit length in the 3D software Amira to facilitate comparisons and to improve the fit of Procrustes analysis and allows analysis of the shapes in the distal and proximal ends (Iqbal 2015) BP/1/4934 was used as the standard and so each specimen was standardized (equalized in length) to that of BP/1/4934. Table (2) shows specimens scale factor. The scale factor represents how many times the specimen was increased or decreased in size to equalized it in length to BP/1/4934.

As models produced using photogrammetry and the laser scanner were used, the difference in resolution created a size difference once the models were imported in Amira. This resolution difference was very large and made digital comparisons of the specimens very difficult. Based on this the decision to scale the specimens was taken. Despite scaling a Procrustes Analysis was still run to ensure that no analytical artefacts would affect the results. The scale factors displayed in Table (2) are more a representation of resolution than they are of life size.

Table (2): A list of the scaling factors used. Positive numbers indicate the specimen was scaled up while negative numbers indicate the specimen was scaled down.

Species	Specimen Number	Scale Factor

Anchisaurus	YPM 1883	220.5
Antetonitrus	BPI/1/4952	15.1
Efraasia	SMNS 12668	109
Massospondylus	BP/1/4934 (Big Momma)	N/A (used at standard) (1)
	BP/1/4732	1.74
	BP/1/4860	1.61
	BP/1/4998a	1.49
	BP/1/4998b	1.5
	BP/1/4999 (proximal)	1.48
	BP/1/4999 (distal)	1.11
	BP/1/5000	1.48
	BP/1/5001	31
	BP/1/5005	1.14
	BP/1/5241 (distal)	1.12
	BP/1/6125	1
	SAM PK 3429	98.5
	SAM PK 5132	50.36
Melanorosaurus	SAM PK 3450	92
	SAM PK 3532	59.3
Pantydraco	BMNH 19 7	568.75
Plateosaurus engelhardti	MBR 4430 163	12.93
	SMNS 12949	38.48
	SMNS 20664	41.91

	SMNS 53537	152.3
	SMNS 91296	46.93
	SMNS 91310	60.32
Plateosaurus gracilis	SMNS 12354	168.27
Plateosauravus	SAM PK 3342	31.31
	SAM PK 3350	87.5
	BPI/1/7358	18
Ruehleia	MBR 4718 104 (proximal)	31.1
	MBR 4718 104 (distal)	37.25
Sefapanosaurus	BPI/1/7434	14.88

Landmarking

The landmarks placed were chosen based on the long-bone scaling patterns study done by Bonnan (2007) on neosauropods and on the muscle reconstructions done by Remes (2008) on Sauropodomorpha.

Many humeri were incomplete or broken into several pieces. To increase the sample size, landmarks were collected in four non-mutually exclusive but analytically discrete sets which reflected specific preservational qualities. These sets are as follows:

- Proximal set - humeri that are complete or retain only a proximal end.
- Distal set - humeri that are complete or retain only a distal end.
- Complete set - humeri that are complete and not broken at the midshaft.
- Fossa set - humeri that preserve a clear olecranon fossa and a clear cuboid fossa.

Proximal Set of Landmarks

This set consists of either complete humeri or humeri that have been broken at the midshaft and retain only a proximal end. The specimens that fit this criteria are found in table (3).

Table (3): List of specimens that are complete or retain only a proximal end

Species	**Specimen Number**
Antetonitrus	BPI/1/4952
Efraasia	SMNS 12668
Massospondylus	BP/1/4934 (Big Momma)
	BP/1/4732
	BP/1/4860
	BP/1/4998a
	BP/1/4998b
	BP/1/4999
	BP/1/5000
	BP/1/5001
Melanorosaurus	SAM PK 3450
	SAM PK 3532
Pantydraco	BMNH 19 7
Plateosaurus engelhardti	MBR 4430 163
	SMNS 12949
	SMNS 20664
	SMNS 53537
	SMNS 91296
	SMNS 91310
Plateosaurus gracilis	SMNS 12354
Plateosauravus	SAM PK 3342
	SAM PK 3350

	BPI/1/7358
Ruehleia	MBR 4718 104
Sefapanosaurus	BPI/1/7434

The landmarks used for this set can be found in table (4) and a diagram of the landmarks can be seen in figure (2). Landmarks 1 and 2 measure the position of the internal tuberosity in relation to the humeral head. Changes in the prominence and angle of the internal tuberosity would change the insertion of subcoracoscapularis (Remes 2008).

Landmarks 2 through 6 measure the convexity of the humeral head and its projection onto the medial and lateral surfaces. Although it is understood that cartilage on the bones can affect the range of motion of the limbs, in non-sauropod sauropodomorphs the shape and extant of articular cartilage is not evident and even conservative estimates are difficult to make hence shape of the structures is used to determine the best possible range of motion. The shape of the humeral head was selected as it has been shown to directly related to maneuverability of the humerus at the gleno-humeral joint(Bonnan and Senter 2007, Remes 2008, Mallison 2010a, Maidment and Barrett 2012). The greater the convexity of the humeral head with a lateral only expansion would promote greater maneuverability of the humerus at the gleno-humeral joint (Bonnan and Senter 2007, Remes 2008, Mallison 2010a). The lateral expansion of the humeral head would, based on work done on Ornithischians, suggest that the humerus would be habitually retracted and could not be extended as a straight forelimb (Maidment and Barrett 2012). A lack of convexity of the humeral head would lead to greater restriction of movement of the humerus in the gleno-humeral joint (Bonnan and Senter 2007, Remes 2008, Mallison 2010a).

Landmarks 7 through 10 measure the prominence and distal elongation of the deltopectoral crest. A more prominent and distally elongated deltopectoral crest indicates a greater cross-sectional area of the deltoideus and pectoralis musculature (Hildebrand and Goslow 2001, Meers 2003, Bonnan 2004, Bonnan 2007, Bonnan and Senter 2007, Remes 2008).

As muscle strength increases with cross sectional area (Meijer 1998, Hutchinson and Garcia2002) this measure can to some extent provide details of the relative muscle strength (Hildebrand and Goslow 2001). The position of the deltopectoral crest relative to the humeral head affects the lever arm and mechanical advantage across the shoulder joint (Hildebrand and Goslow 2001).

A proximally shortened deltopectoral crest indicates that the actions created by the deltoideus and pectoralis, adduction, protraction and retraction (Meers 2003, Bonnan 2004, Remes 2008), have a

greater range of motion but lower mechanical advantage while for more distally elongate deltopectoral crests they have a smaller range of motion but higher mechanical advantage (Bonnan 2004, Remes 2008).

The more distally elongate and expansive deltopectoral crest that create greater force during adduction, protraction and retraction, could indicate an adaption to use the forelimb for stronger grasping motions (Bonnan 2004, Remes 2008)

Table (4): Landmarks used for the proximal dataset

Number	Description	Landmark Type
1	Posterior most tip of internal tuberosity	3
2	Posterior end of humeral head	3
3	Lateral side of humeral head	3
4	Medial side of humeral head	3
5	Anterior end of humeral head	3
6	Geometric middle of humeral head	2
7	Proximal end of deltopectoral projection	3
8	Geometric centre of deltopectoral projection	2
9	Distal end of deltopectoral projection	3
10	Join of deltopectoral crest onto shaft of humerus	3

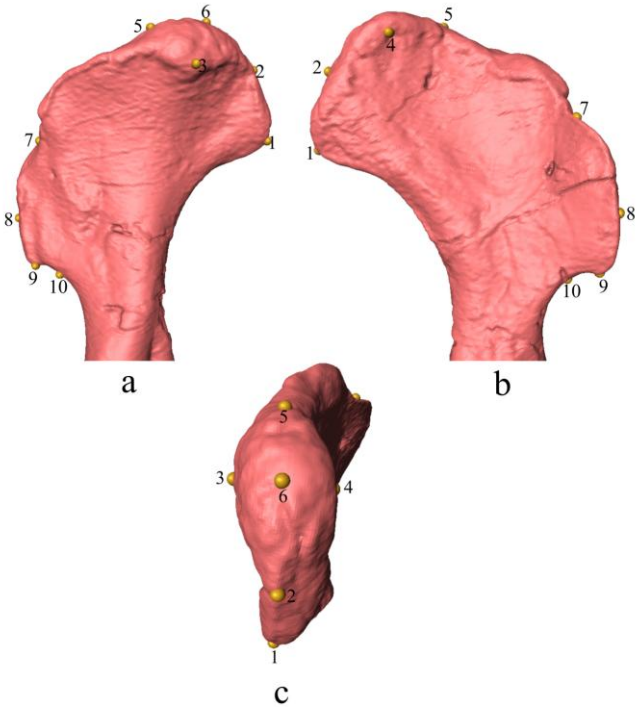

Figure (2): Proximal landmarks of the left humerus used in this study. Reconstructions are of STLs (see methods) as seen in Amira. (a): lateral view; (b): medial view; (c): proximal view. Yellow spheres denote landmark positions. Arabic numerals indicate landmark number (see table (4)). Not to scale

Distal Set of Landmarks

This set consists of either complete humeri or humeri that have broken at the midshaft and retain only a distal end. The specimens that fit this criteria are found in table (5).

Table (5): List of specimens that are complete or retain only a distal end

Species	**Specimen Number**
Anchisaurus	YPM 1883
Antetonitrus	BPI/1/4952
Efraasia	SMNS 12668
Massospondylus	BP/1/4934 (Big Momma)
	SAM PK 3429
	BP/1/4732
	BP/1/4998a
	BP/1/4998b

	BP/1/4999
	BP/1/5000
	BP/1/5001
	BP/1/5005
	SAM PK 5132
	BP/1/5241
	BP/1/6125
Melanorosaurus	SAM PK 3532
Pantydraco	BMNH 19 7
Plateosaurus engelhardti	MBR 4430 163
	SMNS 12949
	SMNS 20664
	SMNS 53537
	SMNS 91296
	SMNS 91310
Plateosaurus gracilis	SMNS 12354
Plateosauravus	SAM PK 3342
	SAM PK 3350
	BPI/1/7358
Ruehleia	MBR 4718 104

All of the landmarks in this set are used to measure the shape and symmetry of the distal humeral condyles as well as their spacing from each other. The landmarks used for this set can be found in table (6) and a diagram of the landmarks can be seen in figure (3).

The distal end of the humerus, in particular the condyles, can be used as a means to interpret the natural articulation and movement of the radius and ulna as well ability to pronate the manus which is important in locomotory assessment (Landsmeer 1983, Remes 2008, Mallison 2010b).

A distinct radial condyle deflection and condyles that are very uneven in shape and widely spaced indicates more maneuverability of the humerus as well as a small amount of ability to pronate the manus (Landsmeer 1983, Bonnan 2003, Remes 2008). Less deflection of the radial condyle and condyles that are more even in shape and more closely spaced indicates less maneuverability of the humerus with little to no ability to pronate the manus (Landsmeer 1983, Bonnan 2003, Remes 2008).

Table (6): Landmarks used for the distal dataset

Number	Description	Landmark Type
1	Geometric middle of the olecranon fossa	2
2	Posterior most point on ulnar condyle	3
3	Lateral most point on ulnar condyle	3
4	Anterior most point on the ulnar condyle	3
5	Geometric middle of the cuboid fossa	2
6	Anterior most point on radial condyle	3
7	Medial most point on radial condyle	3
8	Posterior most point on the radial condyle	3

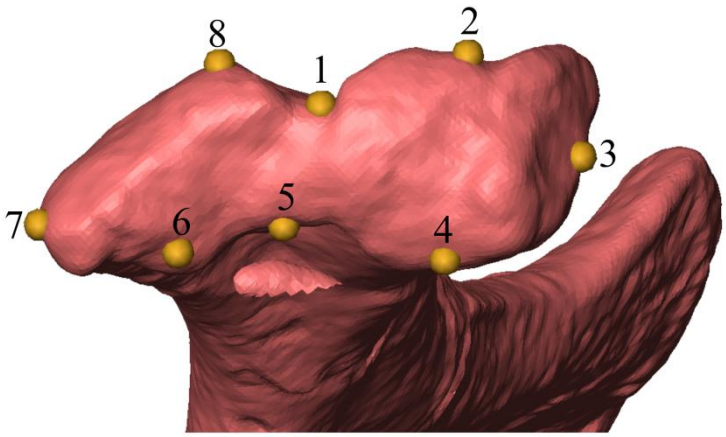

Figure (3): Distal landmarks of the left humerus used in this study. Reconstructions are of STLs (see methods) as seen in Amira. Yellow spheres denote landmark positions. Arabic numerals indicate landmark number (see table (6)). Not to scale

Complete Set of Landmarks

This set consists of specimens that mostly complete and are not broken at the midshaft, retaining both proximal and distal ends. The specimens that fit this criteria are found in table (7).

Table (7): List of specimens that are complete

Species	**Specimen Number**
Antetonitrus	BPI/1/4952
Efraasia	SMNS 12668
Massospondylus	BP/1/4934 (Big Momma)
	BP/1/4732
	BP/1/4998a
	BP/1/4998b
	BP/1/5000
	BP/1/5001
Melanorosaurus	SAM PK 3532
Pantydraco	BMNH 19 7
Plateosaurus engelhardti	MBR 4430 163

	SMNS 12949
	SMNS 20664
	SMNS 53537
	SMNS 91296
	SMNS 91310
Plateosaurus gracilis	SMNS 12354
Plateosauravus	SAM PK 3342
	SAM PK 3350
	BPI/1/7358
Ruehleia	MBR 4718 104

This set of landmarks measures the previous proximal and distal landmarks in relation to each other. These landmarks also allow for the measurement of any torsion in the humeral shaft and the midshaft geometry. The landmarks used for this set can be found in table (8) and a diagram of the landmarks can be seen in figure (4).

Landmarks 1 through 10 deal with the proximal end of the humerus while landmarks 15 to 22 deal with the distal end of the humerus. These are the same landmarks as used previously for the proximal and distal sets. Landmarks 11 to 14 deal with the shape and position of the midshaft of the complete humeri.

Humeral torsion, in this case the relative angle of the distal end to the proximal end, can indicate the amount of supination possible for the forelimb. Humeral torsion, when the antebrachium in placed in a neutral position, allows supination of the manus as seen in theropods and may facilitate grasping motions while less pronounced torsion would facilitate manus pronation during quadrupedal locomotion (Senter and Robins 2005, Senter 2006, Bonnan and Senter 2007, Senter 2007, Remes 2008). To aid in understand torsion the angle of distal end was measured relative to the proximal end in several key specimens. This was done in Amira using digital measurements. A 3D length was applied the proximal end of the humerus straight through the geometric centre of the humeral head. A second line was applied to the distal condyles from landmark 3 to the geometric middle of landmarks

7 and 8. The humerus was then placed in proximal view and the angle of intersection of the two lines measured using the proximal line as the base line.

Table (8): Landmarks used for the complete dataset

Number	Description	Landmark Type
1	Posterior most tip of internal tuberosity	3
2	Posterior end of humeral head	3
3	Lateral side of humeral head	3
4	Medial side of humeral head	3
5	Anterior end of humeral head	3
6	Geometric middle of humeral head	2
7	Proximal end of deltopectoral projection	3
8	Geometric centre of deltopectoral projection	2
9	Distal end of deltopectoral projection	3
10	Join of deltopectoral crest onto shaft of humerus	1
11	Anterior mid shaft	3
12	Lateral mid shaft	3
13	Posterior mid shaft	3
14	Medial mid shaft	3
15	Posterior most point on ulnar condyle	2

16	Lateral most point on ulnar condyle	3
17	Anterior most point on the ulnar condyle	3
18	Geometric middle of the cuboid fossa	3
19	Anterior most point on radial condyle	2
20	Medial most point on radial condyle	3
21	Posterior most point on the radial condyle	3
22	Posterior most point on ulnar condyle	3

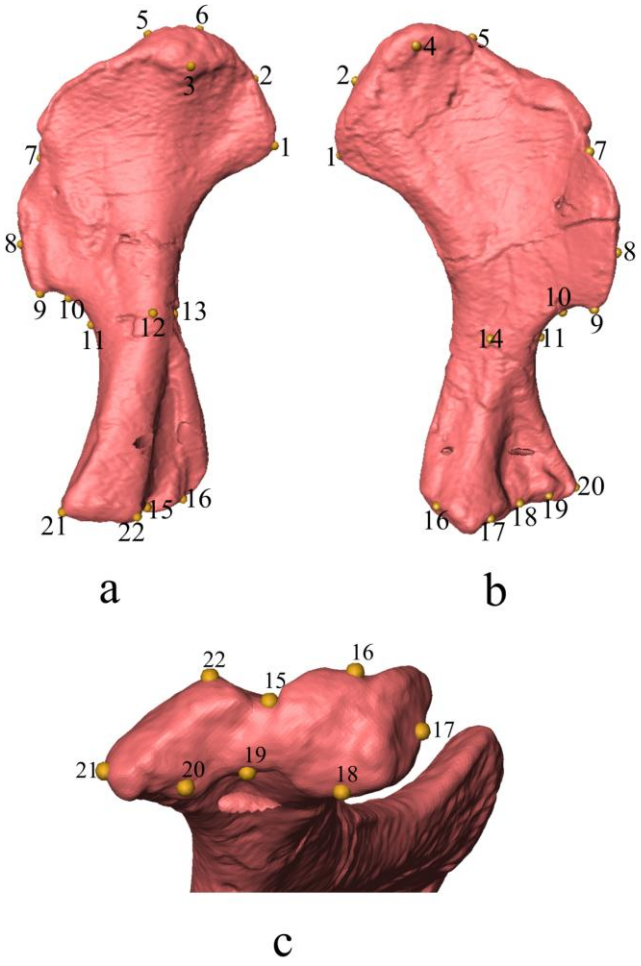

Figure (4): Complete landmarks of the left humerus used in this study. Reconstructions are of STLs (see methods) as seen in Amira. (a): lateral view; (b): medial view; (c): distal view. Yellow spheres denote landmark positions. Arabic numerals indicate landmark number (see table (8)). Not to scale

Fossae Set of Landmarks

This set consists of the specimens that have a clear olecranon and cuboid fossa present on the distal end. Those specimens that do not preserve these features have been excluded from this set. The specimens that fit this criteria are found in table (9).

Table (9): List of specimens that are preserve a clear olecranon and cuboid fossa

Species	**Specimen Number**
Efraasia	SMNS 12668
Massospondylus	BP/1/4934 (Big Momma)
	SAM PK 3429

	BP/1/4998a
	BP/1/4998b
	BP/1/4999
	BP/1/5000
	BP/1/5001
	SAM PK 5132
	BP/1/5241
Melanorosaurus	SAM PK 3532
Plateosaurus engelhardti	MBR 4430 163
	SMNS 12949
	SMNS 20664
	SMNS 53537
	SMNS 91296
	SMNS 91310
Plateosaurus gracilis	SMNS 12354
Plateosauravus	SAM PK 3342
	SAM PK 3350
Ruehleia	MBR 4718 104

This set of landmarks is used to measure the shape and depth of both the olecranon fossa and cuboid fossa on the distal humerus. The landmarks used for this set can be found in table (10) and a diagram of the landmarks can be seen in figure (5).

The relative depth and presence of the cuboid fossa were selected as they can give an indication of the flexion ability of the antebrachium relative to the humerus. A shallower fossa or even no distinguishable fossa would indicate less flexion of the antebrachium is possible while a deeper fossa

would indicate more flexion of the antebrachium is possible. (Bonnan 2003, Bonnan and Senter 2007, Bonnan and Yates 2007).

Derived sauropods which walk in a quadrupedal manner show a lack of the cuboid fossa (Bonnan 2003, Bonnan and Senter 2007, Bonnan and Yates 2007). This would suggest that flexion of the elbow was greatly reduced while extension was complete (Bonnan 2003, Bonnan and Senter 2007, Bonnan and Yates 2007).

Non-sauropodan sauropodomorphs have a clearly defined cuboid fossa that supports a range of forearm flexion similar to theropods (Bonnan and Senter 2007, Bonnan and Yates 2007).

The olecranon fossa seems to be less important in the literature as few papers looking at range of motion use the olecranon fossa (eg., Bonnan 2003, Bonnan and Senter 2007, Bonnan and Yates 2007, Remes 2008, Mallison 2010). However it was decided to assess if any significant shape change occurs in the olecranon fossa and if it can be related back to the olecranon process itself.

Table (10): Landmarks used for the fossa dataset

Number	Description
1	Distal end of the olecranon fosssa on the radial condyle
2	Proximal most point of olecannon fossa
3	Distal end of the olecranon fosssa on the ulnar condyle
4	Geometric centre of olecranon fossa
5	Distal end of the cuboid fosssa on the ulnar condyle
6	Proximal most point of cuboid fossa
7	Distal end of the cuboid fosssa on the radial condyle
8	Geometric centre of cuboid fossa

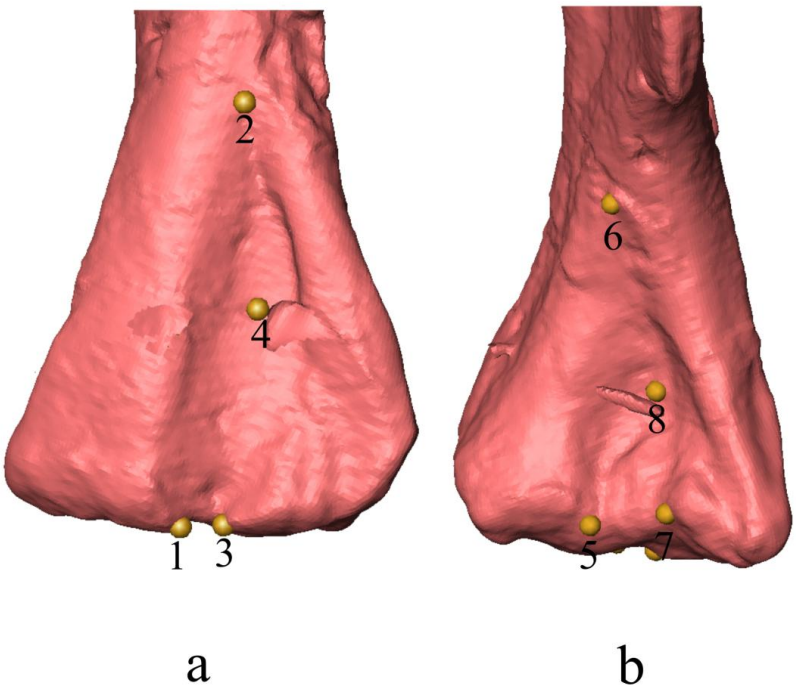

Figure (5): Olecranon fossa and cuboid fossa landmarks of the left humerus used in this study. Reconstructions are of STLs (see methods) as seen in Amira. (a): posterior view; (b): anterior view. Yellow spheres denote landmark positions. Arabic numerals indicate landmark number (see table (10)). Not to scale

Ontogeny Sets

In order to test the hypothesis of postural change during the growth of *Massospondylus*, and to assess humeral shape changes during ontogeny, I focused on specimens of various sizes assumed to be different ontogenetic stages of *M. carinatus* using identical methodology as described above. However a complete set for landmarks could not be done due to the lack of specimens that preserve a complete humerus.

Taxonomic decisions when selecting specimens were taken from the literature or from referrals in the Evolutionary Studies Institute and Iziko South African Museum databases.

In order to divide the specimens into groups based on size, each specimen's proximal-distal length, proximal breadth and distal breadth were measured. Once each specimen has been measured, I looked for a distinctive sizes differences between all the specimens to assign them to a specific group.

Proximal Ontogeny Set of Landmarks

This set included all the *Massospondylus* specimens that were either complete or retained a proximal end. The specimens that fit this criteria are found in table (11).

Table (11): List of *Massospondylus* specimens that are complete or retain only a proximal end

Species	Specimen Number
Massospondylus	BP/1/4934
	BP/1/4860
	BP/1/4988a
	BP/1/4988b
	BP/1/4999
	BP/1/5000

Distal Ontogeny Set of Landmarks

This set included all the *Massospondylus* specimens that were either complete or retained a distal end. The specimens that fit this criteria are found in table (12).

Table (12): List of *Massospondylus* specimens that are complete or retain only a distal end

Species	Specimen Number
Massospondylus	BP/1/4934 (Big Momma)
	SAM PK 3429
	BP/1/4732
	BP/1/4998a
	BP/1/4998b
	BP/1/4999
	BP/1/5000
	BP/1/5001
	BP/1/5005
	SAM PK 5132
	BP/1/5241

	BP/1/6125

Fossae Ontogeny Set of Landmarks

This set included all the *Massospondylus* specimens that were either complete or retained a distal end with a clear olecranon and cuboid fossa. The specimens that fit this criteria are found in table (13).

Table (13): List of *Massospondylus* specimens that preserve a clear olecranon and cuboid fossa

Species	**Specimen Number**
Massospondylus	BP/1/4934 (Big Momma)
	SAM PK 3429
	BP/1/4998a
	BP/1/4998b
	BP/1/4999
	BP/1/5000
	BP/1/5001
	SAM PK 5132
	BP/1/5241

Landmarking Methodology

To ensure consistency in landmark placement, each set was placed on the specimen three times as a separate files in Amira. The individual landmark files were then exported from Amira, saved in the Ascii format and moved into a single folder for each landmark set.

The freeware program R (R Development Core Team 2016) was used to run all analyses. A custom R-script co-written by RBJ Benson and KEJ Chapelle (pers. Comm.) was used to apply geometric morphometric analyses to the 3D landmark data. The script requires the use of two R packages, Abind (Plate and Heiberger 2016) and Morpho (Schlager 2016). The script first looks through the three files generated for each of the three sets of landmarks applied to each specimen to find discrepant

landmarks and using a discriminate value of 92.5% remove them from the dataset, replacing them with an N/A in the data table generated.

After removing the discrepant landmarks the script then averages the remaining values to combine the three files into a single set of averaged values for each landmark position.

Statistical Analysis

After removing discrepant landmarks and averaging the remaining landmarks, statistical tests were run using the same R-script as before which can be found in the appendix. First, a Procrustes superimposition was to minimize scaling and alignment differences between specimens so that remaining variance is only due to shape (Bookstein 1997, Hammer 2002, Zelditch *et al* 2012). This was followed by conducting principal component analyses (PCA) on the Procrustes-adjusted coordinates in order to assess their configurational variation in the sample (Bookstein 1997, Hammer 2002, Zelditch *et al* 2012). Lastly, to test whether the Procrustes analysis effectively removed size variation, I regressed centroid size vs PC1. The expectation is that this regression should not return a significant trend if size has been effectively removed (Bookstein 1997, Hammer 2002, Zelditch *et al* 2012).

In order to test the statistical significance of the ontogeny plots a Goodall's F-test was run using the "testmeanshapes" function of the shapes package in R to test the statistical significance of these plots with regard to the variation between the groups.

The following parameters were used to the run the test and the code can be found in appendix (3)

- resamples - 1000
- replace - false
- scale -true

Limitations

In this study I attempted to sample as widely as feasible across the Sauropodomorpha phylogeny which included 35 specimens across 11 species in which the humerus was considered.

The first major limitation of the study was that only the humerus was sampled. In order to get a more accurate idea of the changes of forelimb morphology and its relation to postural shift , the rest of the forelimb elements, in particular the radius and the ulna, should also be analysed. Many features that

could aid in finding additional evidence of postural shift may appear on other forelimb elements such as the radius and ulna.

The second major limitation of the study was sample size in relation to both the number of species and the number of specimens per species. Many of these specimen are widely spread across many institutions and collections. Travelling to all of these was not possible with the scope of this project and so South American and Asian species were excluded. Preservation also limited what specimens could be used on the study. Specimens that didn't preserve a humerus were immediately excluded and not every specimen that did preserve a humerus was suitable. Some humeri were too deformed or too damaged to create digital models, some broken such that important landmarks were missing and they had to be excluded from the study. Finally not every species is know from more than one specimen. In fact many species are know only from a single type specimen limiting repeatability in the database. By excluding specimens the whole range of the group and any deviations from the normal cannot be fully identified. By sampling more widely this could be fixed.

The third major limitation of this study is the taxonomy of the specimens. Identifying each specimen's correct taxonomy was beyond the scope of this project and so I relied on collection databases and information taken from the literature. However further work on the anatomy of the specimens comparatively could aid in correctly indentifying taxa particularly as I have seen so much intraspecific variation.

Finally only external morphology was examined in this study but internal morphology can be just as important particularly with regard to force distribution in the limb. However the large sample and wide distribution of samples made CT scanning every specimen to examine internal morphology infeasible but a long term study could aid in achieving this.

3.Results

3.1 Proximal Set of Landmarks for all species

This set consists of both complete humeri and humeri that have been broken at the midshaft and retain only a proximal end. The full list of species for this set can found in table (14). Size was effectively removed by the Procrustes analysis, as regressions between PC values and centroid size have low r-squared values (see appendix 2).

Because of the differences in preservational quality, some specimens were missing many landmarks and were excluded from the set. These specimens and a list of which landmarks are missing can be found in appendix 4.

Table (14): Final list of specimens included in the proximal set after exclusion due to missing landmarks.

Species	**Specimen Number**
Antetonitrus	BPI/1/4952
Massospondylus	BP/1/4934 (Big Momma)
	BP/1/4860
	BP/1/4998a
	BP/1/4998b
	BP/1/4999
	BP/1/5000
Pantydraco	BMNH 19 7
Plateosaurus engelhardti	MBR 4430 163
	SMNS 12949
	SMNS 20664
	SMNS 53537
	SMNS 91296
	SMNS 91310

Plateosauravus	SAM PK 3342
	SAM PK 3350
Ruehleia	MBR 4718 104
Sefapanosaurus	BPI/1/7434

In the first run of this set of landmarks two outliers where identified and removed before the set was run again. These outliers where BP/1/4988a and SMNS 91296. Upon examination BP/1/4988a was revealed to have an internal tuberosity that was laterally curved and ended in an extreme point not seen in the corresponding BP/1/4988b and SMNS 91296 has an extremely medially curved deltopectoral crest. These extreme changes are most likely the result of deformation.

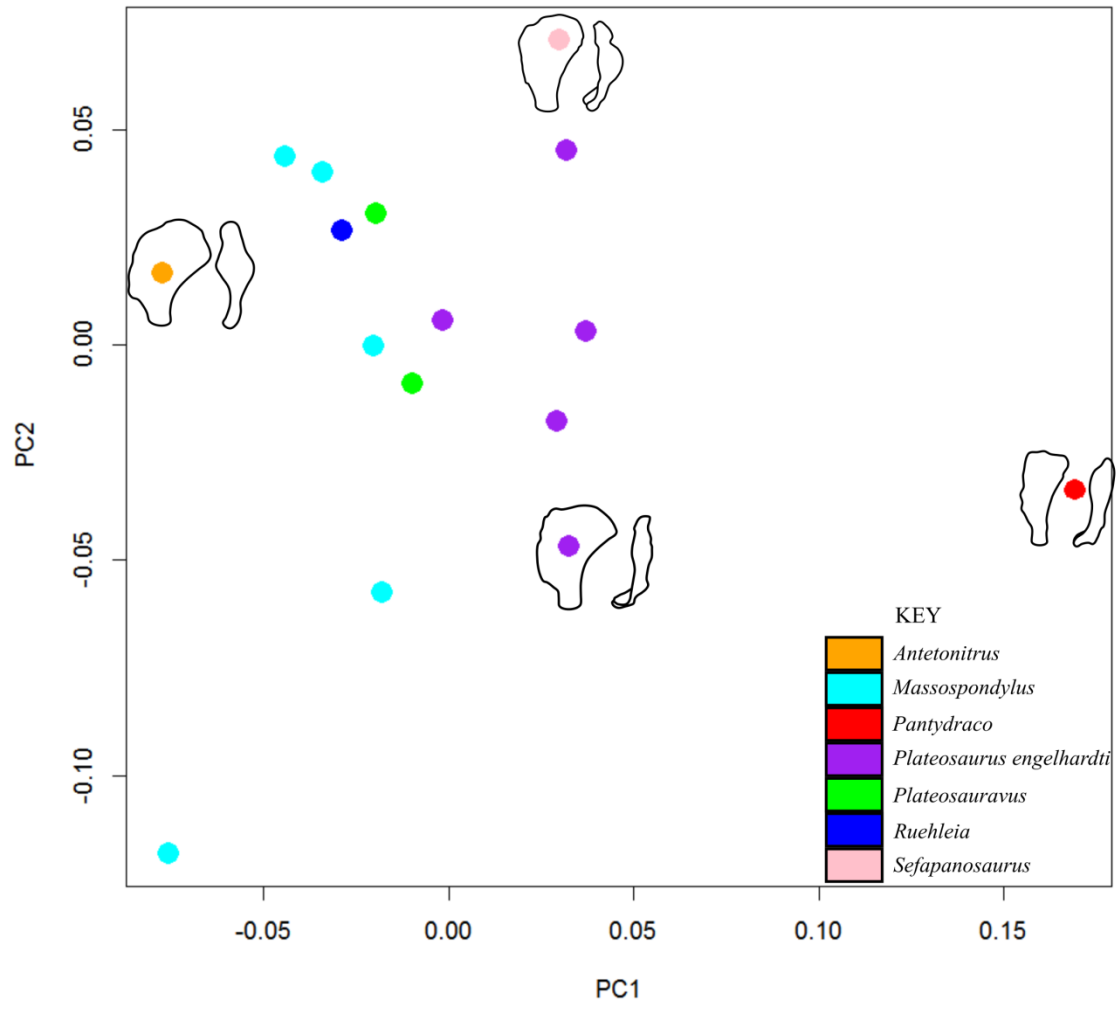

Figure (6): PCA plot of PC1 vs PC2 of the proximal set of landmarks with colour key to indicate species and line drawings indicate the most extreme examples of morphology. PC1 shows (27.02% of variance) describes a change from more domed humeral heads with symmetrical expansions on to the lateral and medial humerus to less domed

heads with a greater lateral expansion and more prominent deltopectoral crests. PC2 (17.82% of variance) seems to be revealing lots of intraspecific variation.

The first principal component (27.02% of variance) clearly separates *Pantydraco* from the rest of the taxa due it radically different morphology very clearly as well as the other taxa while the second principal component (17.82% of variance) seems to be revealing lots of intraspecific variation.

The first principal component axis largely separates taxa along phylogenetic lines, with more derived sauropodomorph taxa with more domed humeral heads that have symmetrical expansions on to the lateral and medial humerus occupying negative positions and basal taxa with less domed heads with a greater lateral expansion and more prominent deltopectoral crests occupying more positive positions along the axis.

Antetonitrus represents the most derived taxon sampled in this analysis. *Antetonitrus* is more negative on PC1 and as such has much more convex humeral head with less projection on the medial and lateral surfaces of the humerus and with a much less anteriorly expansive deltopectoral crest. In comparison *Pantydraco* , which represents the most basal taxon sampled in this analysis, is highly positive on PC1 and has a less prominent humeral head and internal tuberosity but an expansive deltopectoral crest.

Positioned between these two are the rest of the species including *Massospondylus*, *Plateosaurus*, *Plateosauravus*, *Reuhleia* and *Sefapanosaurus*. In the *Massospondylus* group there is one extreme outlier, BP/1/4988b that is highly negative on PC1 and PC2 . BP/1/4988b has, upon further examination, an extremely pointed lateral humeral head expansion.

3.2 Distal Set of Landmarks for all species

This set consists of both complete humeri and humeri that have broken at the midshaft and retain only a distal end. The full list of species for this set can found in table (15). Size was effectively removed by the Procrustes analysis, as regressions between PC values and centroid size have low r-squared values (see appendix 2).

Some specimens were missing many landmarks and were excluded from the set. These specimens and a list of which landmarks are missing can be found in appendix 4.

Table (15): Final list of specimens included in the distal set after exclusion due to missing landmarks.

Species	**Specimen Number**

Anchisaurus	YPM 1883
Efraasia	SMNS 12668
Massospondylus	BP/1/4934 (Big Momma)
	SAM PK 3429
	BP/1/4732
	BP/1/4998a
	BP/1/4998b
	BP/1/4999
	BP/1/5000
	BP/1/5001
	BP/1/5005
	SAM PK 5132
	BP/1/5241
Melanorosaurus	SAM PK 3532
Pantydraco	BMNH 19 7
Plateosaurus engelhardti	MBR 4430 163
	SMNS 12949
	SMNS 20664
	SMNS 53537
	SMNS 91296
	SMNS 91310
Plateosaurus gracilis	SMNS 12354
Plateosauravus	SAM PK 3342

	SAM PK 3350
	BPI/1/7358
Ruehleia	MBR 4718 104

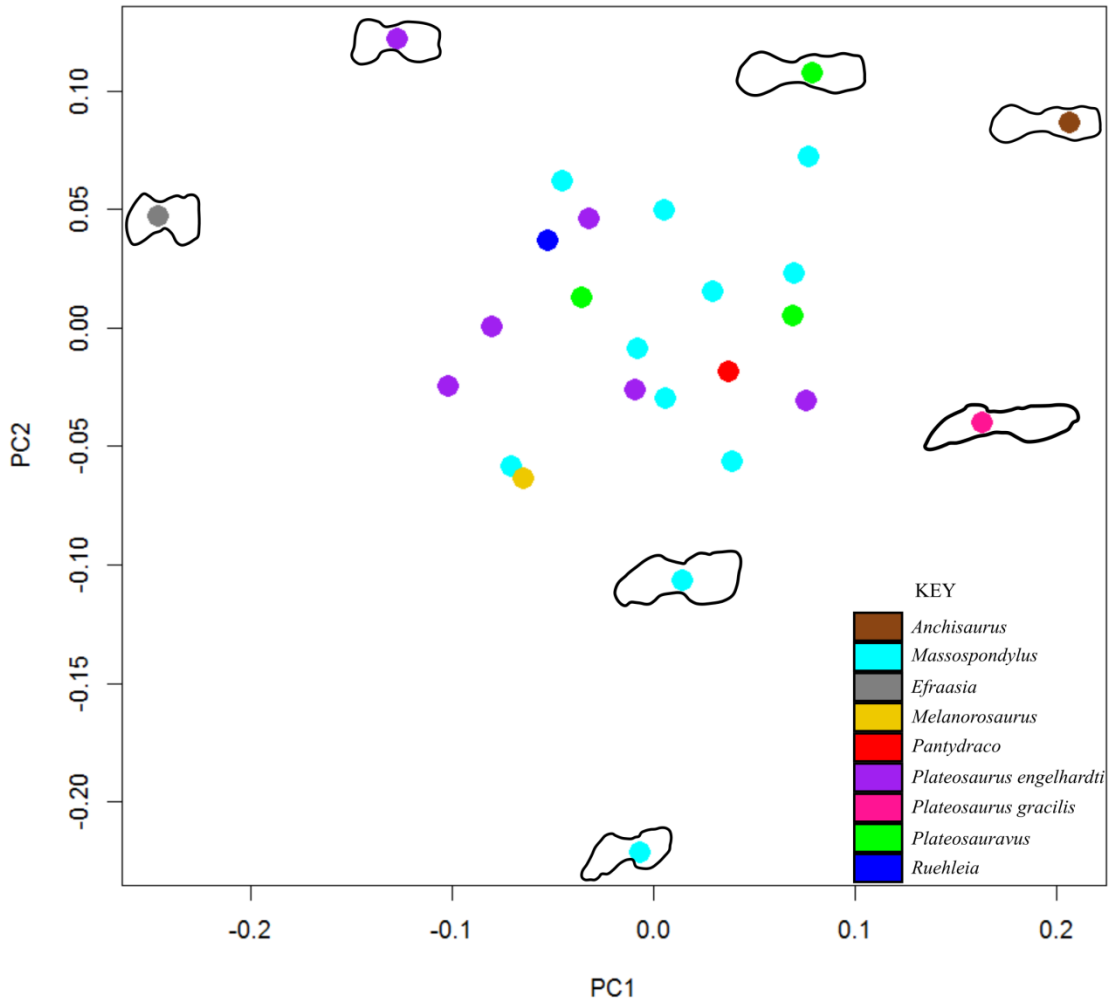

Figure (7): PCA plot of PC1 vs PC2 of the distal set of landmarks with colour key to indicate species and line drawings indicate the most extreme examples of morphology. PC1 (29.82% of variance) describes the change in the deflection of the radial condyle as well as condyle symmetry while PC2 (18.14% of variance) describes the distance between the condyles.

The plot of PC1 vs PC2 for this dataset reveals little clustering by phylogentic relationship. The range of variation within a single taxaonomic entity, such as *Massospondylus*, is general equal to or greater than between entities. Outlying points may be representative of ontogenetic differences or perhaps distortion-related errors.

The first principal component (29.82% of variance) describes the change in the deflection of the radial condyle as well as condyle symmetry while the second principal component (18.14% of variance) describes the distance between the condyles.

The left half of the cluster contains specimens with much less deflection of the radial condyle and condyles that are more even in shape but still relatively widely spaced. The right half of the cluster represents humeri with a distinct radial condyle deflection and condyles that are very uneven in shape and widely spaced.

However there are some outliers. The two largest *Massospondylus* specimens are negative on PC2 and show much more radial deflection than the rest of the *Massospondylus* specimens. The *Plateosaurus* specimens lie close to the same general cluster as the *Massospondylus* specimens again indicating some similarity but again there is an outlying specimen. This *Plateosaurus* specimen is highly positive in on PC2 with almost no radial deflection and relatively symmetrical condyles. This could represent a distortion of the specimen as this particular one, SMNS 91296, has been excluded from the proximal set for its extremely curved deltopectoral crest.

Plateosauravus groups within the cluster as well with one outlier that is highly positive on PC2 with some radial condyle deflection and relatively asymmetrical condyles. *Efraasia* is also highly positive on PC2 and highly negative on PC1. It shows little radial condyle deflection and has condyles that are relatively close and slightly more symmetrical. *Anchisaurus* is highly positive on PC1 and PC2. It shows some radial deflection and condyles that as relatively distant and asymmetrical. *Plateosaurus gracilis* is highly positive on PC1 and shows a large amount of radial deflection with nonsymmetrical condyles that are relatively distant.

PCA's were run again with all juveniles specimens excluded for both proximal and distal plots to ensure that ontogenetic and phylogenetic signals were not confused (see appendix (5)). There was very little difference between the plots that have juveniles and those that don't. Indeed the distal plot with the juveniles excluded is almost identical to the original plot that contains juveniles. This clearly shows that the inclusion of juvenile taxa is not skewing the results in any significant way and so phylogenetic and ontogenetic signals are not being confused.

3.3 Complete Set of Landmarks for all species

This set consists of bones that mostly complete and are not broken at the midshaft, retaining both proximal and distal ends. The full list of species for this set can found in table (16). Size was effectively removed by the Procrustes analysis, as regressions between PC values and centroid size have low r-squared values (see appendix 2). Some specimens were missing many landmarks and

were excluded from the set. These specimens and a list of which landmarks are can be found in appendix 4.

Table (16): Final list of specimens included in the complete set after exclusion due to missing landmarks.

Species	**Specimen Number**
Massospondylus	BP/1/4934 (Big Momma)
	BP/1/4998a
	BP/1/4998b
	BP/1/5000
Pantydraco	BMNH 19 7
Plateosaurus engelhardti	MBR 4430 163
	SMNS 12949
	SMNS 20664
	SMNS 53537
	SMNS 91296
	SMNS 91310
Plateosauravus	SAM PK 3342
	SAM PK 3350
Ruehleia	MBR 4718 104

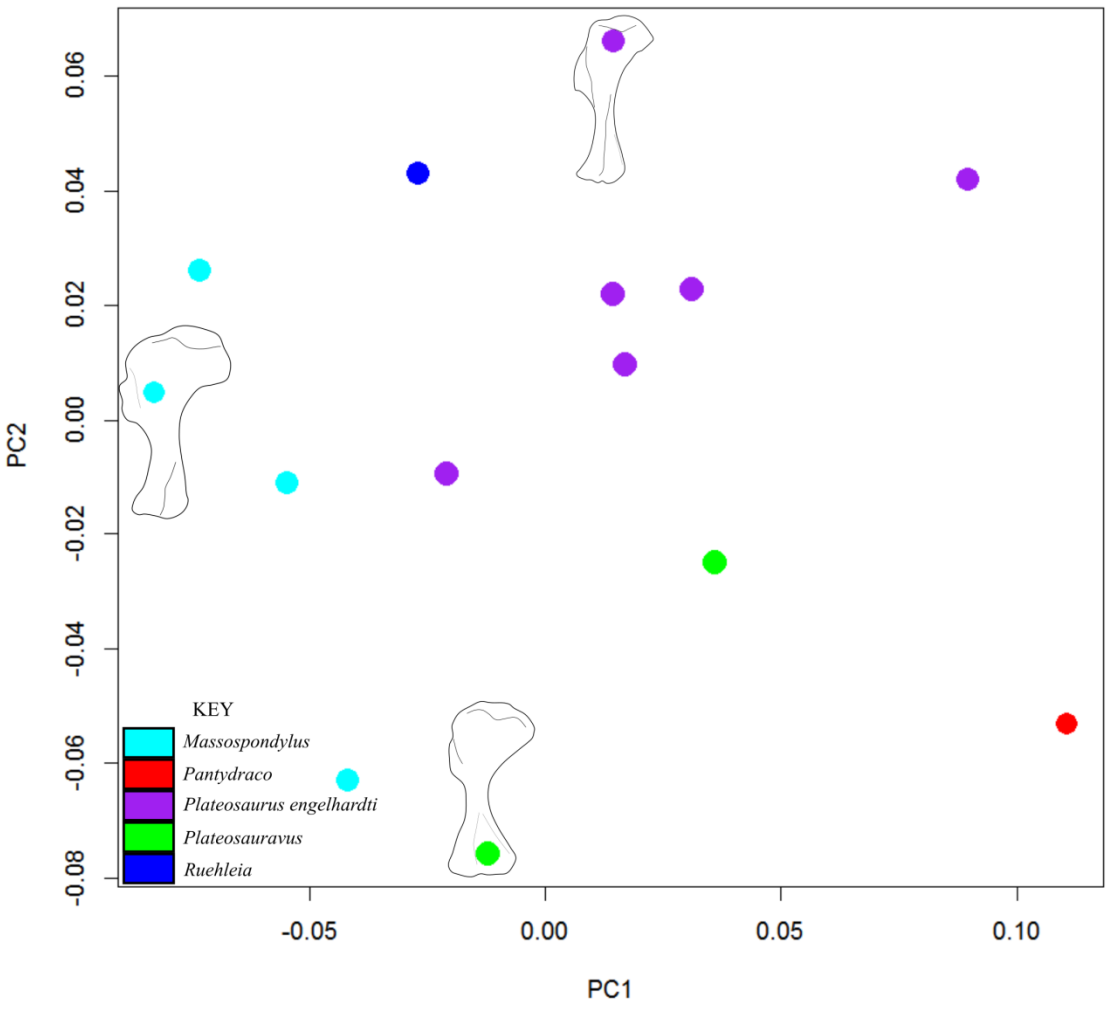

Figure (8): PCA plot of PC1 vs PC2 of the complete set of landmarks with colour key to indicate species and line drawings indicate the most extreme examples of morphology. . PC1 (35.12% of variance) describes a reduction in the convexity of the humeral head, its projection on to the medial and lateral surfaces of humerus, the increasing prominence and distal elongation of the deltopectoral crest, and increasingly more symmetrical distal ends with less deflection of the radial condyle. PC2 (19.61% of variance) describes the increasing twist in the humeral shaft as well as a change from a short, stocky humeral shaft to a longer, more slender shaft.

Both the first principal component and the second principal component separate out the species present in this analysis into discrete groups. Each taxon does have a distinct humeral shape, and within each taxon there is still a large amount of intraspecific variability, although intrataxon differences seem lower than intertaxon differences.

The first principal component (35.12% of variance) mostly describes a reduction in the convexity of the humeral head, its projection on to the medial and lateral surfaces of humerus, the increasing prominence and distal elongation of the deltopectoral crest, and increasingly more symmetrical distal

ends with less deflection of the radial condyle. A general phylogenetic trend can be observed along PC1 from relatively more derived to relatively more basal.

The second principal component (19.61% of variance) describes the increasing twist in the humeral shaft as well as a change from a relatively short and stocky humeral shaft to a relatively longer and more slender shaft. The general phylogenetic trend can be seen here from basal to more derived with one outlier from *Massospondylus* group that is highly negative compared to the rest of the group.

Massospondylus appears to have the has the less anterioposteriorly expansive deltopectoral crest that is proximally short when compared with *Plateosaurus*. However *Massospondylus* still has an expansive deltopectoral crest when compared with more derived sauropodomorphs. *Massospondylus* also has asymmetrical distal condyles with a distinct deflection of the radial condyle while *Plateosaurus* has symmetrical condyles with no deflection of the radial condyles. All the groups present in this sample display some degree of humeral torsion which are displayed in appendix 4. In general *Plateosaurus* show more humeral torsion then *Massospondylus*. *Plateosaurus* shows, on average, a distal end that is rotated 32° to 40° relative to the proximal end while *Massospondylus* shows a distal end that is rotated 28° to 34° relative to the proximal end. *Pantydraco* shows less torsion than the other specimens with a distal end that is rotated 12° relative to the proximal.

3.4 Fossae Set of Landmarks for all species

This set consists of the specimens that have a clear olecranon and cuboid fossa present on the distal end. Those specimens that do not preserve these features have been excluded from this set. The full list of species for this set can found in table (13). Size was effectively removed by the Procrustes analysis, as regressions between PC values and centroid size have low r-squared values (see appendix 2).

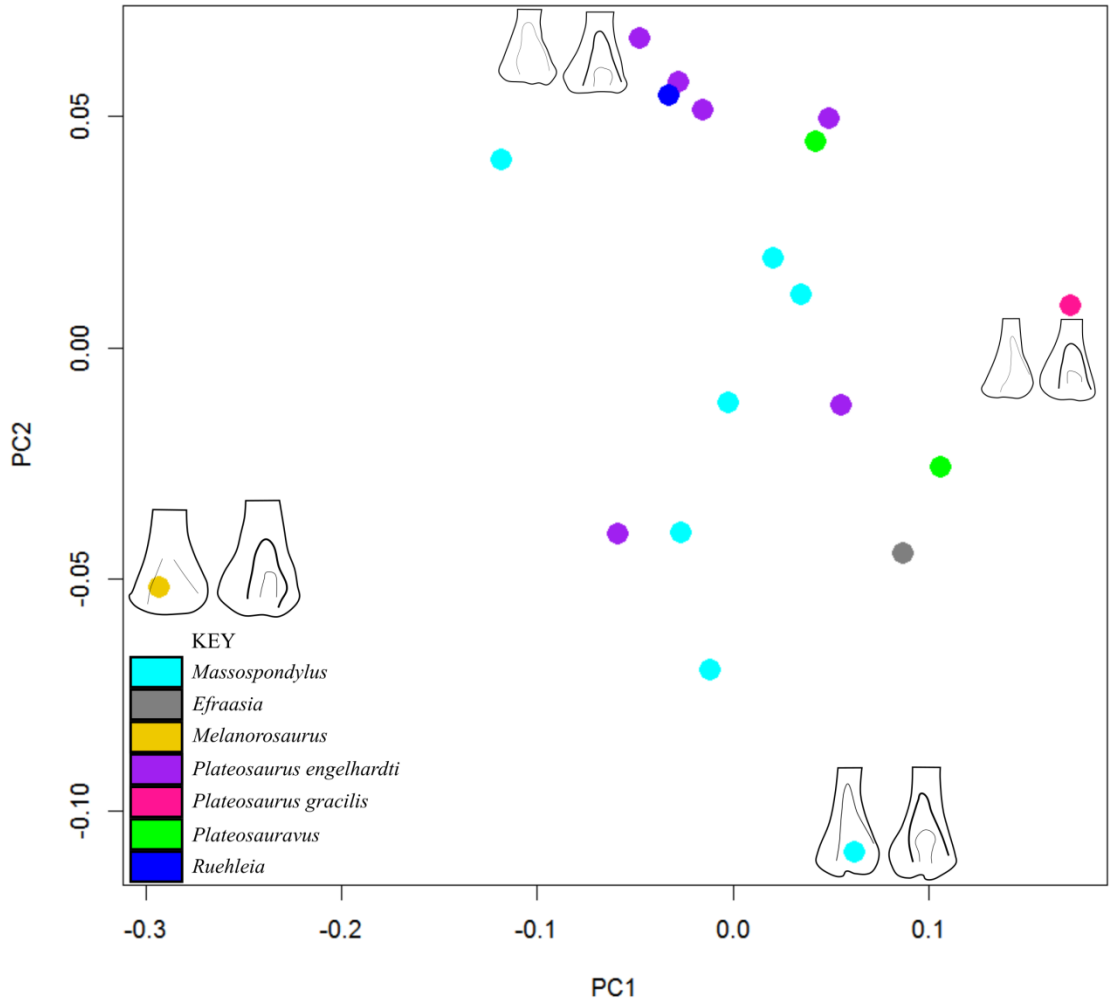

Figure (9): PCA plot of PC1 vs PC2 of the olecranon and cuboid fossa of the distal humerus landmarks with colour key to indicate species and line drawings indicate the most extreme examples of morphology. . PC1 (48.22% of variance) shows of the cuboid fossa from relatively deep to relatively shallow. PC 2 (12.93% of variance) shows variation of the olecranon fossa from very shallow and poorly defined to deep and very well defined.

This data set has appears to have no clear grouping and reveals a lot of variation of the olecranon fossa and little variation of the cuboid fossa.

In figure (9) the first principal component (48.22% of variance) explains variation of the cuboid fossa from relatively deep to relatively shallow. Most of the specimens seem to sit in a very narrow range of PC1 from -0.1 to 0.1. This would indicate there is very little change in the cuboid fossa. *Melanorosaurus* would be the exception from this trend with an exceptionally deep cuboid. *P.gracilis* has the most shallow cuboid fossa and also falls outside the group but only just. The group that falls within the -0.1 to 0.1 all have similar relatively deep cuboid fossa.

The second principal component (12.93% of variance) mostly explains variation of the olecranon fossa from very shallow and poorly defined to deep and very well defined. There does not appear to be any phylogenetic pattern but rather a large amount of variation not only between species but within species as well.

Overall it seems there is little variation of the cuboid in the groups present. There is a lot of variation in the olecranon fossa both between species and in terms of interspecies variation as well.

3.5 Proximal Ontogeny Set of Landmarks

The measurements of each specimen were recorded into table (17). The measurements were then used to divide the specimens into the significantly larger adult specimens and the smaller sub adult specimens. With regards to using size to determine the ontogenetic stage of the specimens, I assumed that the taxa information from the various intuitions was correct as identifying the taxon of each specimen was beyond the scope of this project. This means that I used size relative to BP/1/4934 as a way to assign age. Chinsamy (1993) has previous used histology of the femur to estimate growth rates of *Massospondylus* specimens and concluded that relative size can be used to indicate age.

When first and second principal components were plotted against logged centroid size and a regression line was plotted it was found that the r-squared values for both were low (appendix 2) indicating that remaining variance was due to shape. However with no predictable relationship, due to low r-squared values, it means that there may not be concerned changes in shape due to size differences.

Table (17): Measurements taken for each specimen in the set to determine relative size groups

Specimen	**Proximal-Distal Length (cm)**	**Proximal Breadth (cm)**	**Group Assigned**
BP/1/4934	26	13.5	Adult
BP/1/4860	N/A	8.2	Sub adult
BP/1/4988a	17.4	9	Sub adult
BP/1/4988b	17.2	9.2	Sub adult
BP/1/4999	N/A	9.2	Sub adult
BP/1/5000	23	13.1	Adult

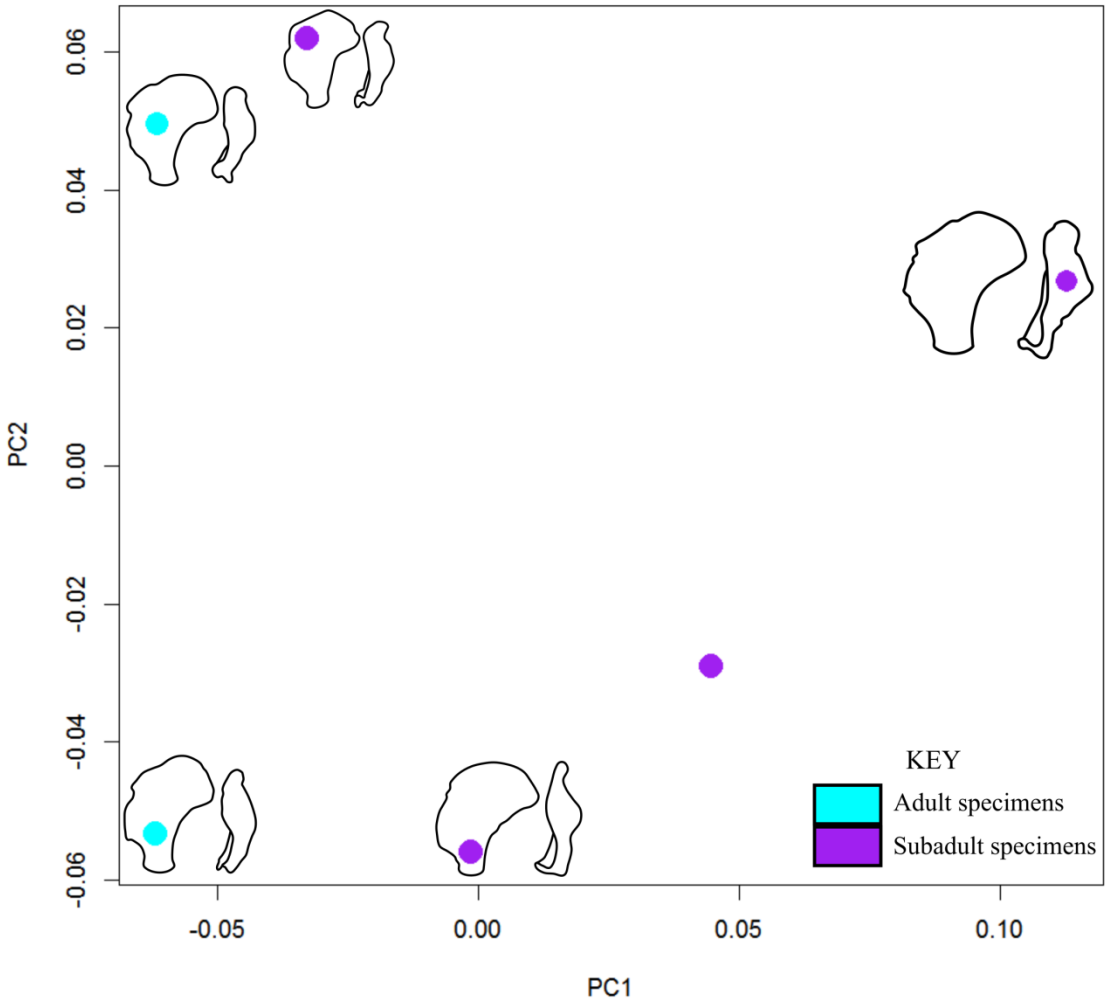

Figure (10): PCA plot of PC1 vs PC2 of the proximal set of ontogeny landmarks with colour key to indicate size group and line drawings indicate the most extreme examples of morphology. . PC1 (47.76% of variance) describes a reduction in the convexity of the humeral head and its projection on to the medial and lateral surfaces of humerus. PC2 (28.20% of variance) describes the decreasing prominence and proximal shortening of the deltopectoral crest and a change in the internal tuberosity from relatively thin to relatively thick mediolaterally.

The first principal component (47.76% of variance) describes a reduction in the convexity of the humeral head and its projection on to the medial and lateral surfaces of humerus. The second principal component (28.20% of variance) seems to describe the decreasing prominence and proximal shortening of the deltopectoral crest as well as a change in the internal tuberosity from relatively thin to relatively thick mediolaterally.

The adult specimens have relatively more convex humeral heads and both of the adults have a less expansive lateral expansion onto the lateral side of the humerus. The subadult specimens have a much greater lateral expansion of the humeral head but much less convexity.

The deltopectoral crest seems to have a lot of variation between adult and sub adult. Specimens plotting in more negative positions on PC2 have a more distally elongated and prominent deltopectoral crest the more positive specimens on PC2 have a more proximally shortened and less prominent deltopectoral crest.

The group of adult specimens seems to show great variation in their internal tuberosity from relatively thin to relatively thick medio-laterally. The group of sub adult specimens again show much variation in their internal tuberosity.

3.6 Distal Ontogeny Set of Landmarks

The measurements of each specimen were recorded into table (18). The measurements were then used to divide the specimens into the significantly larger adult specimens and the smaller sub adult specimens.

When first and second principal components were plotted against logged centroid size and a regression line was plotted it was found that the r-squared values for both were low (appendix 2) indicating that remaining variance was due to shape. However with a limited predictable relationship, due to a low r-squared value of 0.403, it means that there may not be concerned changes in shape due to size differences.

Table (18): Measurements taken for each specimen in the set to determine relative size groups

Specimen	**Proximal-Distal Length (cm)**	**Distal Breadth (cm)**	**Group Assigned**
BP/1/4934	26	8.6	Adult
SAM PK 3429	N/A	5.6	Sub adult
BP/1/4732	N/A	5.4	Sub adult
BP/1/4988a	17.4	6.5	Sub adult
BP/1/4988b	17.2	6.6	Sub adult
BP/1/4999	N/A	7.5	Sub adult
BP/1/5000	23	9.9	Adult
BP/1/5001	N/A	6	Sub adult

BP/1/5005	N/A	7.2	Sub adult
SAM PK 5132	N/A	11	Adult
BP/1/5241	N/A	6.9	Sub adult

BP/1/4988a was removed as outlier point from the plot after the first analysis. This specimen has now appeared as an outlier on several plot. The PCA was then rerun excluding this point.

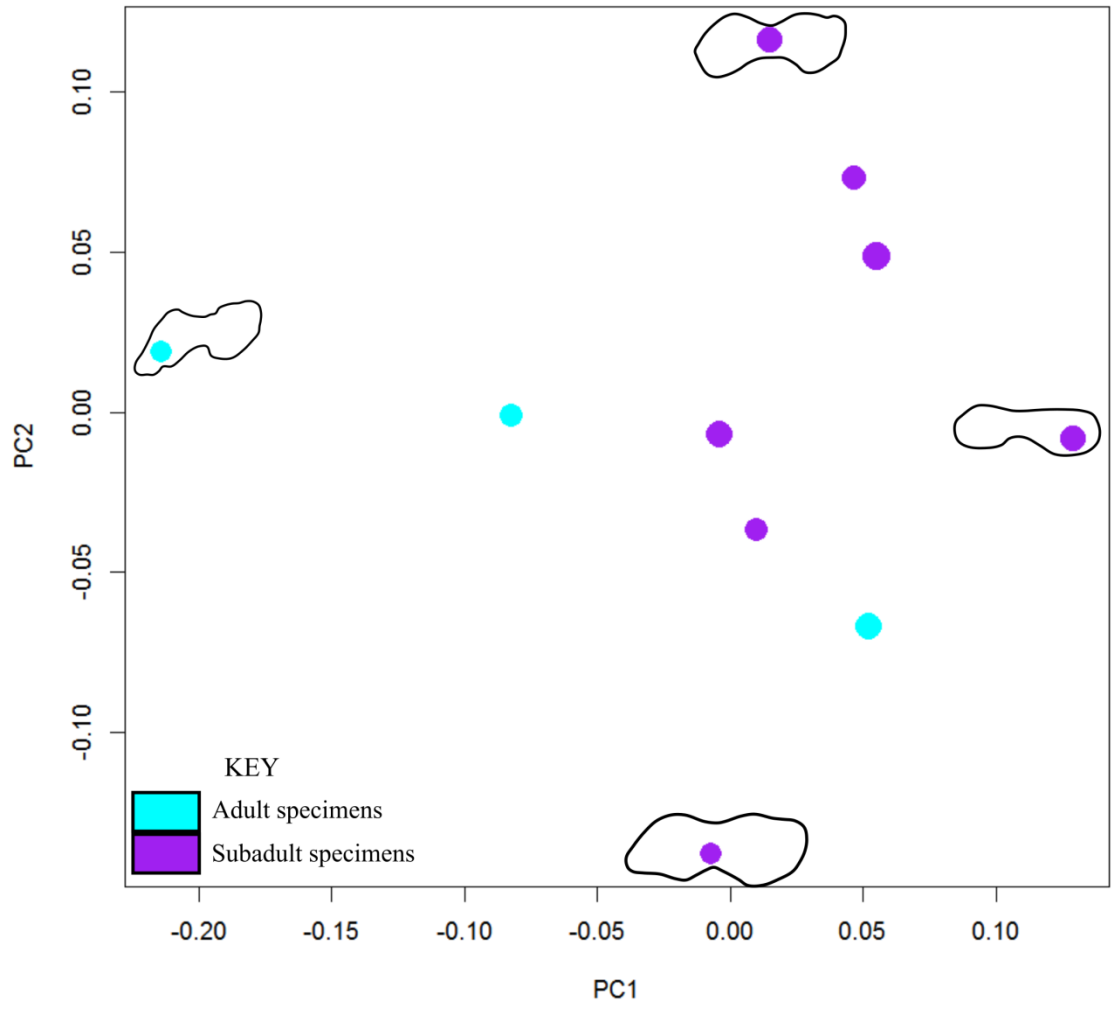

Figure (11): PCA plot of PC1 vs PC2 of the distal set of ontogeny with colour key to indicate size group and line drawings indicate the most extreme examples of morphology. . PC1 (40.26% of variance)describes a change from the most deflected radial condyle with the condyles being nonsymmetrical. PC2 (24.24% of variance) describes a change from closely spaced condyles to more widely spaced condyles.

The first principal component (40.26% of variance)describes a change from the most deflected radial condyle with the condyles being nonsymmetrical. The second principal component (24.24% of variance) describes a change from closely spaced condyles to more widely spaced condyles.

There is a clear distinction in that the two largest specimens, BP/1/4934 and SAM PK 5132, are clearly separated by their radial condyle deflection. BP/1/5000, a larger specimen, has a shape more similar to the smaller humeri. It displays less radial condyle deflection than the rest of the larger specimens and has less nonsymmetrical condyles that are more closely spaced than the other larger specimens.

The group of smaller specimens show a lot of variation in their condyle spacing but are very similar in the minor deflection to almost no deflection of the radial condyle. The second smallest specimen SAM PK 3429 has the least amount of radial deflection indicating a lessened ability to pronate the hand.

3.7 Fossa Ontogeny Set of Landmarks

The measurements of each specimen were recorded into table (19). The measurements were then used to divide the specimens into the significantly larger adult specimens and the smaller sub adult specimens.

When first and second principal components were plotted against logged centroid size and a regression line was plotted it was found that the r-squared values for both was exceptionally low indicating that remaining variance was due to shape (appendix 2). However with no predictable relationship, due to low r-squared values, it means that there may not be concerned changes in shape due to size differences

Table (19): Measurements taken for each specimen in the set to determine relative size groups

Specimen	**Proximal-Distal Length (cm)**	**Distal Breadth (cm)**	**Group Assigned**
BP/1/4934	26	8.6	Adult
SAM PK 3429	N/A	5.6	Sub adult
BP/1/4999	N/A	7.5	Sub adult
BP/1/5000	23	9.9	Adult
BP/1/5001	N/A	6	Sub adult

SAM PK 5132	N/A	11	Adult
BP/1/5241	N/A	6.9	Sub adult

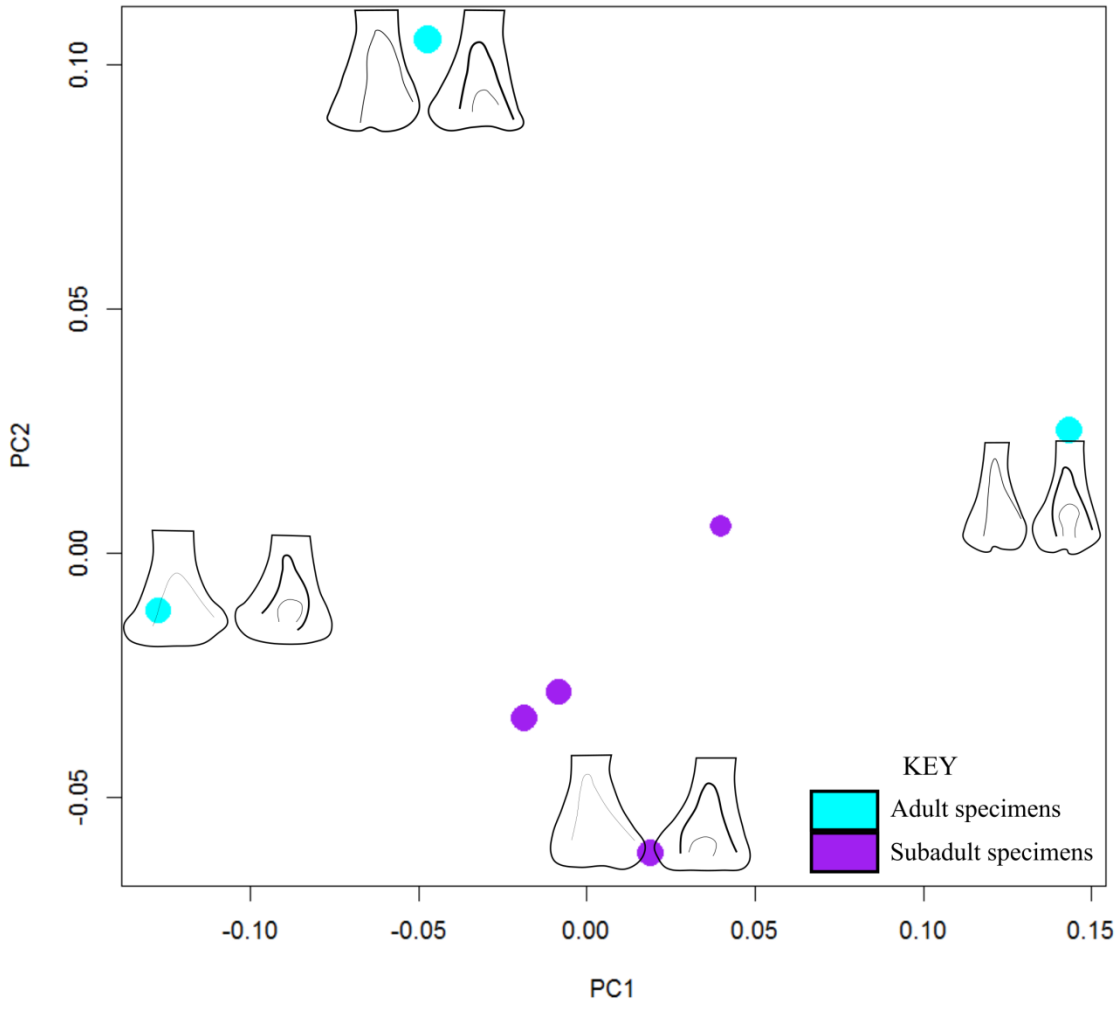

Figure (12): PCA plot of PC1 vs PC2 of the fossae set of ontogeny landmarks with colour key to indicate size group and line drawings indicate the most extreme examples of morphology. . PC1 (45.03% of variance) explains the change in the shape and depth of the olecranon fossa from very shallow with a more rounded proximal apex to very deep, well bounded with a sharp proximal apex. PC2 (19.11% of variance) mostly explains the change in the cuboid fossa which remains deep.

In figure (12) the first principal component (45.03% of variance) mostly explains the change in the shape and depth of the olecranon fossa from very shallow with a more rounded proximal apex to very deep, well bounded with a sharp proximal apex.

The second principal component (19.11% of variance) mostly explains the change in the cuboid fossa. Interestingly the cuboid fossa itself seems to undergo very little change, remaining relatively deep throughout all the specimens in this set though the smaller specimens have a slightly shallower cuboid fossa.

Results of Goodall's F-Test on the ontogeny sets

Table (20): Results of Goodall's F-test

Set of Landmarks	**P-value**	**Table P-value (F-statistic)**
Proximal set	0.1148851	0.2422089
Distal Set	0.1648352	0.1366779
Fossae Sets	0.000999001	0.08956353

The p-value obtained for the proximal and distal sets indicates that the differences between the adult group and subadult group are not statistically significant. The p-value obtained for fossae set indicates that the differences between the adult group and subadult group are statistically significant. However looking at the F-statistic, assuming several conditions that this data set may violate, indicates that the adult group and subadult group are not statistically significant.

4.Discussion

Overall, this study looked at 35 humeri across a broad range of non-sauropodan Sauropodomorphs. From these data, I am able to draw preliminary conclusions that there is shift in the morphology of the humerus that indicates shapes characteristic of sauropods begin to evolve relatively early in the sauropodomorph lineage. The basal most sauropodomorphs and basal non-sauropodan sauropodomorphs display humeral morphology consistent with obligate bipedalism while the most derived non-sauropodan sauropodomorphs display humeral morphology consistent with both habitual bipedalism and facultative quadrupedalism and once the eusauropods are reached the humerus shows clear modification for obligate quadrupedal locomotion. The ontogeny of the humerus of *Massospondylus* points to the adult specimens being able to exhibit habitual bipedalism with facultative quadrupedalism.

4.1 Shape changes of the humerus across the sauropodomorph lineage and their implications for posture and gait

Across the lineage of Sauropodomorpha the humerus shows concerted morphological change and these changes in shape are likely due to increased quadrupedality as they increase in body mass.

Proximal Humerus

Alterations of the proximal humerus, in particular the humeral head and the deltopectoral crest, are among the most distinctive and consistent shape changes across the phylogeny. Two prominent morphological differences can be followed from the basal-most sauropodomorphs to the most derived non-sauropodan sauropodomorph, *Antetonitrus*: 1) a change in convexity of the humeral head from less convex in the basal-most sauropodomorphs to more convex in progressively more crownward taxa; and 2) differences in the length and prominence of the deltopectoral crest from distally elongate that are more anteriorly expansive to proximally shortened that are less anteriorly expansive. I discuss these individually below.

Humeral head

The humeral head changes from less convex with a stronger lateral projection onto the humeral shaft in the more basal taxa to more convex with weak projections onto both the medial and lateral surfaces of the humerus in more crownward taxa (figure (6)). *Pantydraco*, which represents the most basal taxon sampled in this analysis, has a less prominent humeral head that is extremely hard to discern. This may be due to *Pantydraco* being a juvenile specimen (Yates 2003) and on the principle component plots (figure (6)) it plots a distance away from the other species. This is similar to the subadult *Massospondylus* specimens in the lack of humeral head convexity but little else. *Plateosaurus*, slightly more crownward than *Pantydraco* but still relatively basal within the clade, has

much less doming of the humeral head. *Antetonitrus,* the most derived taxon in this analysis, has a much more convex humeral head with less projection on the medial and lateral surfaces of the humerus as can be seen in figure (6).

Increased humeral head convexity can be correlated with greater maneuverability of the humerus at the gleno-humeral joint (Bonnan and Senter 2007, Remes 2008, Mallison 2010a). This is certainly true in primates where a more convex humeral head increases the range of motion of the humerus at the gleno-humeral joint (Rose 1989, Larson 1995). Therefore, the lack of convexity of the humeral head could indicate that their humerus was restricted in its motion in the gleno-humeral joint (Bonnan and Senter 2007, Remes 2008, Mallison 2010a). The lateral expansion of the humeral head would, based on work done on Ornithischians, suggest that the humerus would be habitually retracted and could not be extended as a straight forelimb in quadrupedal Ornithischians (Maidment and Barrett 2012).

Greater extension of the limb would have been required for quadrupedalism in large sauropods in order to achieve a columnar posture (Bonnan 2003). In sauropods the olecranon process is also reduced or completely absent which also indicated greater extension of the forelimb was possible. This indicates that the humeral head, when it is more convex and has no lateral expansion, would allow the forelimb to extend to a greater degree (Maidment and Barrett 2012). The shallowness of the olecranon fossa could also indicates a reduced olecranon process further supporting that greater extension of the forelimb is possible in derived sauropods (Bonnan 2003). In this sample I saw the increasing convexity of the humeral head as well as the loss of the lateral expansion that could indicate that the humerus was able to extend the forelimb to a greater degree in more derived members of the lineage.

Deltopectoral crest

The deltopectoral crest changes in both prominence and proximodistal elongation as seen in figure (6). A more prominent and distally elongated deltopectoral crest indicates a greater cross-sectional area of the deltoideus and pectoralis musculature (Remes 2008, Maidment and Barrett 2012) as seen in the basal-most sauropodomorphs. Progression along the phylogeny towards more derived non-sauropodan sauropodomorpha has the deltopectoral crest becoming less prominent and proximally shortened.

In contrast, quadrupedal ornithischians seem to display the opposite trend where more derived ornithischians show the more prominent and proximodistally elongated deltopectoral crest (Maidment and Barrett 2012). Maidment and Barrett (2012) reached this conclusion by examining and measuring key taxa from the ornithiscian lineage.

Although most true sauropods have a reduced deltopectoral crests, brachiosaurids have an anteriorly directed and prominent deltopectoral crest that extends over slightly more than one third of the humerus (Rauhut 2006). This could be an indication of the greater force needed to move their large forelimbs during locomotion (Bonnan 2003).

The shortening and decrease in prominence of the deltopectoral in more derived non-sauropodan sauropodomorphs leads to a change in the mechanical advantage of the shoulder joint. Based on Maidment and Barrett's (2012) reconstructions of ornithscicians, and Remes (2008) reconstructions of sauropodomorphs it can be observed that the proximally shorter deltopectoral crest moves the insertions of the deltoideus and pectoralis closer to their origins. With shorter deltopectoral crests, the actions created by the deltoideus and pectoralis, which insert on the deltopectoral crest and perform the actions of adduction, protraction and retraction, will have a greater range of motion with less mechanical advantage (Hildebrand and Goslow 2001, Meers 2003, Remes 2008). Greater range of motion rather than greater force generation of the forelimb could indicate an adaption to a more quadrupedal gait (Bonnan 2004, Remes 2008). As with mammals that increase greatly in body mass, quadrupedal sauropods adopt a columnar posture (Biewener, 1989, VanBuren and Bonnan 2013). This adoption of a more columnar limb would have also meant a reduction of the locomotor abilities in sauropods (Carrano 2005, Rauhut *et al* 2011). In derived sauropods a proximodistally shorter deltopectoral crest suggests that the sites of the muscles that insert on the deltopectoral crest would be located closer to the humeral head so decreasing the amount of force that acted upon the humerus (Bonnan 2004).

In contrast the more distally elongate and expansive deltopectoral crest of more basal non-sauropodan sauropodomorphs creates greater force during adduction, protraction and retraction (Hildebrand and Goslow 2001, Meers 2003, Remes 2008). Greater mechanical advantage rather than a greater range of motion in the forelimb could indicate an adaption to a for a bipedal gait with strong grasping capabilities (Bonnan 2004, Remes 2008).

Internal tuberosity

The internal tuberosity showed considerable intraspecific variation while no phylogenetic pattern was discernible on the principle component plot (figure (6)). Changes in the prominence and angle of the internal tuberosity would change the insertion of subcoracoscapularis and so in order to attempt to investigate this landmarks were included that covered the internal tuberosity. (Remes 2008). However the intraspecific variation and variation between species made any changes unreliable for interpretation. The internal tuberosity varied across *Massospondylus* from mediolaterally thick to mediolaterally thin and its orientation varied with no pattern across *Massospondylus* and over species from more medially curved to more laterally curved. While the curve changes could simply be from distortion, the changing thicknesses are perplexing as it is neither related to ontogeny nor phylogeny.

Distal humerus

The major changes in shape of the distal humerus relate to the humeral condyles. More basal non-sauropodan sauropodomorphs such as *Efraasia* and *Plateosaurus* have more symmetrical condyles (figure (7)) that are more closely spaced with little to no posterior deflection of the radial condyle. In contrast, the more derived non-sauropodan sauropodomorphs, such as *Massospondylus*, have more widely spaced, asymmetrical condyles where the radial condyle is distinctly posteriorly deflected (figure (7)).

Asymmetry of the distal condyles and spacing of the condyles has functional relevance for manus pronation (Landsmeer 1983, Bonnan 2003, Remes 2008). Those taxa with more symmetrical condyles may have relatively little ability to pronate the manus, and those with deflection of the radial condyle may have improved mobility about this joint for the radius and ulna, and thus are able to pronate the manus (Landsmeer 1983, Bonnan 2003, Remes 2008). This allows the hand to rotate into a putatively propulsive orientation, which would in part facilitate the power stroke necessary for locomotion.

While the deflection of the radial condyle, particularly in the larger specimens, of *Massospondylus* would indicate some degree of pronation, further analysis of other features such as the large degree of humeral torsion (see below) and the convexity of the humeral head would indicate this is not true or ability to pronate the manus was very minor. Most recent studies on *Massospondylus* seem to indicate that pronation was impossible (Bonnan and Senter 2007).

Pronation of the manus has implications for quadrupedalism (Hildebrand and Goslow 2001, Bonnan 2003; Bonnan and Senter 2007, Bonnan and Yates 2007). In order to be able to walk in a quadrupedal manner the palmer or ventral surface of the manus must be pronated to contact the ground and produce propulsive forces (Hildebrand and Goslow 2001, Bonnan 2003; Bonnan and Senter 2007, Bonnan and Yates 2007).

All members of Sauropoda are hypothesized to have walked with a pronated manus, which would have provided efficiency gains in quadrupedal locomotion (Bonnan 2003, Bonnan and Senter 2007). Thus, the lack of shape modifications in non-sauropodan Sauropodomorphs for manual pronation suggests that this evolved later on the tree, and in fact its absence may effectively rule out habitual quadrupedalism.

Most of the non-sauropodan sauropodomorphs in this sample display little distal adaptation for pronation of the manus. *Efraasia* and *Plateosaurus* both have features of the distal humerus consistent with no manus pronation ability which would indicate they are bipedal if manus pronation is an indication for quadrupedalism (Hildebrand and Goslow 2001, Bonnan 2003; Bonnan and Senter 2007, Bonnan and Yates 2007).

The most interesting feature here is the ability of *Massospondylus* to potentially pronate its manus as this is thought to be impossible even in the juveniles (Reisz *et al* 2012). While the smaller specimens of *Massospondylus* are consistent with this idea having little to no posterior radial deflection. The two largest specimens both have a distinctive posterior radial deflection which would indicate some ability to pronate the manus. *Melanorosaurus,* a more derived specimen, also shows a slight posterior deflection of the radial condyle though to a lesser extent. Bonnan and Yates (2007) speculated that *Melanorosaurus* was at least facultatively quadrupedal based on mosaic of sauropod and non-sauropodan sauropodomorphs features of its forelimb. The similarity in the radial condyle could indicate that this was also the case for *Massospondylus* - they were habitually bipeds that could move in slow quadrupedal posture if needs be as speculated by Bonnan and Senter (2007).

Complete humeri

Analysis of the complete humeri yielded results similar to those obtained from proximal and distal elements, albeit with lower sample size, as well as giving an idea of the amount of torsion of the humerus as can be seen in figure (8).

Proximal and distal ends

The most basal non-sauropodan sauropodomorph taxa (*Pantydraco, Plateosaurus*) in the sample had the most anteriorly expansive and least proximodistally short deltopectoral crest with its distal condyles being the most symmetrical, again showing little posterior deflection of the radial condyle (figure (8)).

Massospondylus as the second most derived non-sauropodan sauropodomorph in the this sample had the least anterioposterioly expansive and most proximodistally shortened deltopectoral crest with its distal condyles being the most asymmetrical, showing a posterior deflection of the radial condyle (figure (8)).

Humeral torsion

Humeral torsion is the relative angle of the distal end to the proximal end of the humerus. Various grades of torsion are present in all specimens for this sample, though this seems to lessen across the phylogeny from basal to derived (Figure (8)). In the PC1 vs PC2 plot (Figure (8)) the various species are well partitioned based on various characters that were measured such as the deltopectoral crest and distal condyles (see above). They are also spread out across PC2 based on humeral torsion.

Plateosaurus has a greater degree of humeral torsion than *Massospondylus* . *Plateosaurus* shows, on average, a distal end that is rotated 32° to 40° relative to the proximal end while *Massospondylus* shows a distal end that is rotated 28° to 34° relative to the proximal end. It is important to note

however that *Massospondylus* still has a significant degree of humeral torsion especially when compared with even more derived sauropods such as *Cetiosauriscus* that shows almost no humeral torsion. (Tschopp *et* al 2015).

Pantydraco strangely does not follow this trend as it had a much lower degree of humeral torsion compared the rest of the sample - only 12° of distal end rotation relative to the proximal end. This may be due to *Pantydraco* being a juvenile specimen and this is a feature on ontogeny. Indeed the *Massospondylus* species that are classed as subadults display less humeral torsion than the adult specimen on this plot.

Functionally, humeral torsion can give an indication of the amount of supination possible for the forelimb (Senter and Robins 2005, Senter 2006, Bonnan and Senter 2007, Senter 2007, Remes 2008).Humeral torsion, when the antebrachium in placed in a neutral position, allows supination of the manus as seen in theropods and may facilitate grasping motions while less pronounced torsion would facilitate manus pronation during quadrupedal locomotion (Senter and Robins 2005, Senter 2006, Bonnan and Senter 2007, Senter 2007, Remes 2008).

That all these specimens have a degree of humeral torsion would indicate they were capable of grasping motions. *Antetonitrus,* though both specimens not including due to one missing its radial condyle and the other being too damaged, still displays a noticeable amount of humeral torsion. When the *Antetonitrus* specimen BPI/1/4952 was measure it was found to have a distal end that was rotated approximately 37° relative to the proximal end. This is comparable to the amount of humeral torsion seen in *Plateosaurus,* much higher than expected. *Efraasia* had the highest degree of torsion, 53° though this may be due to some distortion on the specimen. However this high degree is expected for more basal Sauropodomorpha. *Cetiosauriscus* however has almost no humeral torsion which is expected as it is an obligate quadruped (Meyer and Thüring 2003). As supination is facilitated by humeral torsion (Senter and Robins 2005, Senter 2006, Bonnan and Senter 2007, Senter 2007, Remes 2008), these higher degrees of torsion indicate that even the more derived non-sauropodan sauropodomorphs are retaining some degree of bipedality as they become more derived while true sauropods lose this ability altogether.

Fossae

The olecranon fossa shows a lot of variation, but this variation does not seem to reflect phylogenetic patterns on the principle component plot (figure (9)). The cuboid fossa is invariant in its shape across the specimens sampled. This result was surprising, as these fossae are thought to play a role in flexion and extension of the antebrachium in relation to the humerus. I explain in greater detail below.

Olecranon Fossa

The olecranon fossa in mammals is widely thought to receive the olecranon process of the ulna to allow the forearm to extend (Rich and Vickers-Rich 2000). However, Fujiwara *et al* (2010) however looked at forearm function in modern birds and crocodiles and concluded that the olecranon fossa does not, in fact, receive the olecranon process in these taxa. Rather, the smaller intercotyle process of the ulna is received by the fossa in these taxa. Using extant phylogenetic bracketing, Fujiwara *et al* (2010) assumed that could also be the case for dinosaurs.

In derived sauropods the condition of the olecranon fossa is extremely shallow or barely present (Bonnan 2003, Carrano 2005). For example, my personal observations on *Cetiosauriscus* showed that this basal sauropod had only a shallow, barely discernible olecranon fossa. This is supported by published observations on other sauropod taxa: e.g., *Haestasaurus* (Upchurch *et al* 2015)

The olecranon fossa varies widely in its morphology in Sauropodomorpha. For example, within *Massospondylus*, it ranges from being a shallow, barely discernible depression to a deep, groove-like feature (figure (9)). This may be due to either ontogenetic or taphonomic factors or these samples could be different taxa.

Cuboid Fossa

The cuboid fossa however showed little shape variation across the phylogeny and was present in all specimens bar one (figure (9)). The cuboid fossa is functionally related to the flexion ability of the antebrachium relative to the humerus. The two exceptions to this were *Melanorosaurus* and *Plateosaurus gracilis. Melanorosaurus* displays a very deep and proximodistally long cuboid fossa while *Plateosaurus gracilis* has an extremely shallow cuboid fossa. *Melanorosaurus* clearly retains, despite being more derived, a degree of elbow flexion similar to more basal non-sauropodan sauropodomorphs indicating it may have retained some degree of bipedality. *Plateosaurus gracilis* appears to have been mediolaterally compressed a great deal. The bone also appears flat and this may explain why the fossa is so shallow rather than function implication.

The retention of a relatively deep cuboid fossa is a feature shared with bipedal basal Sauropodomorpha and more derived theropods such as *Allosaurus* (Bonnan 2003, Bonnan and Senter 2007, Langer *et al* 2007). Though Burch (2014) states that this feature is present in most theropods, she noted its lack of presence as distinctive feature in very basal theropods such *Tawa hallae*. Maidment and Barett (2011) also noted that it is not present in basal ornithischians. The retention of this feature in Sauropodomorpha, and its shape-invariant nature, supports the hypothesis that they retained high degrees of antebrachial flexion. This in turn indicates that even if they were using quadrupedal gaits, they retained the ability to use the forelimb in ways more characteristic of bipeds.

<u>Comparisons with more derived sauropods</u>

Compiling a complete dataset for Sauropodomorpha which included derived sauropods was unfortunately outside of the scope of this study. However, I was able to inspect *Cetiosauriscus*, a basal diplodocoid, and a paper on another specimen of *Cetiosauriscus* (Meyer and Thüring 2003) to verify key aspects of humeral anatomy in Sauropoda (Tschopp *et* al 2015).

There are stark differences in humeral morphology between non-sauropodan sauropodomorphs and even the most basal sauropods. In sauropods, the deltopectoral crest is reduced in proximodistal length and is far less prominent. These changes may indicate that retraction, protraction and adduction are lower in mechanical advantage in sauropods but have a greater range of motion – a shift that can be directly related to locomotor efficiency (Hildebrand and Goslow 2001, Bonnan 2004, Remes 2008). The distal condyles of the examined *Cetiosauriscus* are somewhat damaged and reconstructed and so telling their original shape is difficult but there does seem to be some degree of asymmetry between the radial and ulnar condyle. In terms of humeral torsion *Cetiosauriscus* displays almost no torsion, with the axes of the proximal and distal ends being parallel. This is presumed to aid in pronation of the manus during quadrupedal locomotion (Senter and Robins 2005, Senter 2006, Bonnan and Senter 2007, Senter 2007, Remes 2008). Both the olecranon fossa and the cuboid fossa are barely visible. The cuboid fossa being so shallow as to be almost nonexistent indicated that range of forearm flexion is limited (Bonnan 2003, Bonnan and Senter 2007). The olecranon fossa is also extremely shallow with no distinct bounding indicating that extension of the forearm was increased (Bonnan 2003, Bonnan and Senter 2007). *Cetiosauriscus* clearly has a humerus that is modified for quadrupedal locomotion. This and its phylogenetic position as a basal diplodocid make it a good point of comparison for the less derived and thought to be bipedal non-sauropodan sauropodomorphs.

Summary of shape changes in the sauropodomorph humerus across the phylogenetic tree

In summary, these data support shifts in both proximal and distal humeral morphology on the line leading to Sauropoda. In general, the basalmost sauropodomorph taxa have a humeral head this is flat and broad, a proximodistally long and more anteroposteriorly prominent deltopectoral crest, more humeral torsion and a deep cuboid fossa. More derived non-sauropodan sauropodomorphs have a humeral head that is more convex but that extends only a short ways laterally, a proximodistal short and less anteroposteriorly prominent deltopectoral crest, less but a lower amount of humeral torsion and a deep cuboid fossa that is still present.

My observations show that these trends continue into true sauropods, where the humeral head is even more convex, the deltopectoral crest is proximodistally short and less anteroposteriorly prominent, the humerus lacks torsion and a cuboid fossa is no longer present. *Massospondylus, Melanorosaurus* and *Antetonitrus,* as more derived non-sauropodan sauropodomorphs show mixed features of both quadrupeds and bipeds. For example, *Antetonitrus* has a very reduced deltopectoral crest but still has distinct humeral torsion and a deep cuboid fossa.

The morphology of the humerus indicates shapes characteristic of true sauropods (and reflecting their particular locomotory style of quadrupedalism) began to evolve relatively early in the sauropodomorph lineage. Thus, the evolution of quadrupedality may have been a slow, stepwise process involving gradual changes in the humeral head, deltopectoral crest, torsion of the humeral shaft, and reduction of the cuboid fossa. However, it may be that some of these features, such as a greater range of motion in the humeral head, evolved for reasons not directly involved in quadrupedal gaits (e.g., foraging efficiency). In that case, these morphological changes are good examples of exaptations which were later co-opted to enable large body size.

4.2 Humeral shape change during the ontogeny of Massospondylus

Massospondylus is thought to change it posture through its ontogeny (Reisz *et al* 2005) from a quadrupedal hatchling to a bipedal juvenile and adult. Although this idea has been supported by some trackways and allometric regressions (Livingston *et al* 2009), I attempted to quantify this using morphology of the humerus as an independent means of assessment.

The proximal morphology of the humerus was consistent with what I expected to find and can be seen on the principle component plot of figure (10). The smaller specimens had a less anterioposteriorly prominent deltopectoral crest that was proximally shorter with less convex humeral head. The larger specimens have a more distally elongate and anterioposteriorly expansive deltopectoral crest with a more convex humeral head. These differences do not appear to be due to differential ossification though some distortion of the direction of the curve of the deltopectoral crests is presents.

The distal end of the humerus was more interesting in its assessment. While all the specimens have asymmetrical condyles and display the some radial condyle deflection contrary to expectations the largest specimens show the greatest amount of radial condyle deflection while the smaller specimens have less radial condyle deflection (figure (11)). This is different to expected results were the smallest specimens should have had a posterior radial condyle deflection to facilitate quadrupedalism (see below).

There is little change in the cuboid fossa but the smaller specimens have a slightly shallower cuboid fossa than the larger specimens while the olecranon fossa is more variable though only the largest specimens have a distinct and deep fossa (figure (12)).

In terms of the changes of the proximal humerus the more distally elongate and expansive deltopectoral crest of the larger specimens creates greater force during adduction, protraction and retraction of the humerus, indicating an adaption to use the forelimb for stronger grasping motions (Hildebrand and Goslow 2001, Bonnan 2004, Remes 2008). The internal tuberosity varies greatly between specimens of all sizes from from relatively thin to relatively thick mediolaterally but it

particularly notable in the adult specimens (figure (10)). Therefore thickness of the internal tuberosity is not as reliably correlated with ontogenetic stage for *Massospondylus*.

In terms of the changes of the distal humerus with so many specimens having asymmetrical condyles and displaying the radial condyle deflection with this being greatest in largest specimens indicates that both large and small specimens had a very minor degree of pronation of the manus but it was greater in larger specimens (figure (11)). This is contrary to what was expected for these data in which I thought to find greater pronation of the manus of the smaller species and less pronation of the manus in the larger specimens. Both Reisz *et al* (2012) and Bonnan and Senter (2007) have indicated that young *Massospondylus* could not pronate their manus at all despite being hypothesized as quadrupedal and were walking in a inefficient manner before switching to bipedalism as adults. This means that the smallest specimens are in line with Reisz *et al* (2012) predications of no pronation in the young *Massospondylus* despite quadrupedal posture. The adults should not show any ability to pronate their manus but they do, indicating they have potential to adopt a quadrupedal posture as predicted by Bonnan and Senter (2007).

The differences in the fossae indicate that the larger specimens with a deeper cuboid (figure (12)) would have greater flexion of the antebrachium based in this observation but the smaller specimens would still a good degree of flexion (Bonnan 2003, Bonnan and Senter 2007). This may also indicate decrease in muscle forces generated by young individuals or to the lack of complete ossification of the diaphysis in young individuals.

The internal tuberosity has a large amount of variation in thickness mediolaterally, therefore thickness of the internal tuberosity is not as reliably correlated with ontogenetic stage. BP/1/4934 also shows some distortion of its distal end that places it as an outlier on this plots.

BP/1/4988a has been an outlier point on several plots but it became very clear with the *Massospondylus* plots that this specimen is distorted. BP/1/4988a has very odd pointed projections of internal tuberosity and radial condyle. BP/1/4988a and BP/1/4988b are a pair of left and right humeri from the same animal. Neither of features are present BP/1/4988b. This leads to the conclusion that this is distortion. The distortion of its condyles caused it to be removed from the distal ontogeny set as it was placed extremely positively on the PC2 axis, well away from the rest of the specimens.

The changes in the proximal humerus morphology indicate that the larger specimens could produce greater forces during adduction, protraction and retraction of the humerus, indicating an adaption to use the forelimb for stronger grasping motions (Hildebrand and Goslow 2001, Bonnan 2004, Remes 2008). The distal humerus indicates that despite the young *Massospondylus* being quadrupedal they had little degree of pronation of manus while the larger specimens had a greater degree of manus pronation indicating they have been capable of some degree of quadrupedality (Bonnan and Senter

2007). The continued presence of the cuboid fossa indicates that all of the specimens had a good degree of flexion of the antebrachium (Bonnan 2003, Bonnan and Senter 2007).

The f-tests (table (20)) run on these data revealed that the differences are not statistically significant in the proximal and distal sets. While the fossae are statistically significant further investigation and use of the f-statistic revealed that the differences are not statistically significant and so caution is advised for this set. However this may be due to the very small sample that was used. It is also possible that the some of the subadult specimens are just small adults and this is why the differences are not significant in the qualitative sense. Quantitatively some difference can be seen between the specimens but whether this is taxonomic differences or the results of small amounts of distortion is unclear and the case of taxonomy is beyond the scope of this project.

4.3 Is paedomorphosis implicated in the locomotory evolution of Sauropoda?

If paedomorphosis were driving the evolution of quadrupedality in Sauropoda, one would expect to find that juvenile *Massospondylus* specimens, which thought to be are quadrupedal (Reisz *et al* 2012), would have at least some of the suite of features I previously noted in taxa like *Cetiosauriscus*. For example, one might expect that juvenile *Massospondylus* specimens would have reduced deltopectoral crests, highly convex humeral heads, and asymmetrical distal condyles with distinct amounts of posterior radial condyle deflection. My observations suggest a few similarities, but show overall that juvenile *Massospondylus* were likely not using the same sorts of quadrupedal gaits which more derived sauropods used.

Some of the morphology of the proximal humerus is quite similar between sauropods and juvenile *Massospondylus*. The expansion of the deltopectoral crest in the adult specimens is similar to the basal most sauropodomorphs while the smaller specimens, which have a less expansive deltopectoral crest, are similar to derived non-sauropodan sauropodomorphs.

The distal humerus indicated that specimens of all sizes could pronate the manus to some degree and the cuboid fossa was present and deep in all specimens meaning flexion of the antebrachium has a range comparable to theropods (Bonnan and Senter 2007). This presents an ambiguous idea as to whether or not adults were either entirely bipedal or entirely quadrupedal. This seems to agree with the literature which identifies the adults as possibly both bipedal and quadrupedal though bipedal is favoured as the mostly likely gait (Bonnan and Yates 2007, Bonnan and Senter 2007, Remes 2008) and does not clearly answer the question of retention of juvenile characters.

In order to more fully answer this question a larger sample size of *Massospondylus* with good taxonomic identification is required as well data procured from several derived sauropods. Adding in the forelimb of the embryos would also aid in finding this answer especially as negative allometry has

already been established for *Massospondylus* (Livingston *et al* 2009). While they are hard to come by the ontogeny of other species of Sauropodomorpha could shed further light on this issue especially if using histology to age the specimens such as Klein and Sander (2007) who investigated the bone growth history of *Plateosaurus* with this method.

5.Conclusion

Shapes of the humerus characteristic of sauropods, although subtle, begin to evolve relatively early in the sauropodomorph lineage, before the appearance of obligate quadrupedality. This suggests a protracted, stepwise process in the macroevolutionary trajectory that led to the evolution of sauropodan graviportal posture, possibly involving some functional tradeoffs (e.g., limited mobility of the limb) in order to support to the larger body weights of eusauropods.

Basalmost sauropodomorphs and basal non-sauropodan sauropodomorphs, such as *Efraasia* and *Plateosaurus,* display humeral morphology consistent with obligate bipedalism such as a prominent deltopectoral crest, a larger degree of humeral torsion, and more symmetrical condyles. Later-branching non-sauropodan sauropodomorphs in this study, such as *Melanorosaurus, Massospondylu*s and *Antetonitrus,* display humeral morphology that could be used for facultative quadrupedalism such as a more rounded humeral head, a less prominent deltopectoral crest, a lesser degree of humeral torison, and asymmetrical condyles. Eusauropods (although not a major component of this work) show humeral modification for obligate quadrupedal locomotion.

A shift from juvenile quadrupedality to adult bipedality has been proposed for *Massospondylus*, but the data analyzed here show little similarity between its humeral ontogenetic trajectory and that seen in the lineage leading to derived sauropods. This strongly suggests that quadrupedality in sauropods is not a paedomorphic retention of an early-stage locomotory strategy, but rather a derived, de-novo feature unique to that clade. Moreover, this suggests that *Massospondylus* had its own unique shift in locomotory strategy, and only future ontogenetic studies can assess how widespread that pattern was.

Future work should include increasing the number of species, particularly with regard to the eusauropods, that are included in the study. Furthermore, additional forelimb elements should be also be added into this study, particularly the radius and manus elements. Additional future studies of posture could use CT scanning to investigate internal bone structure and determine where the major forces are applied in the limb bones.

Appendix 1 - PC2 vs PC3 plots for all Landmark Sets

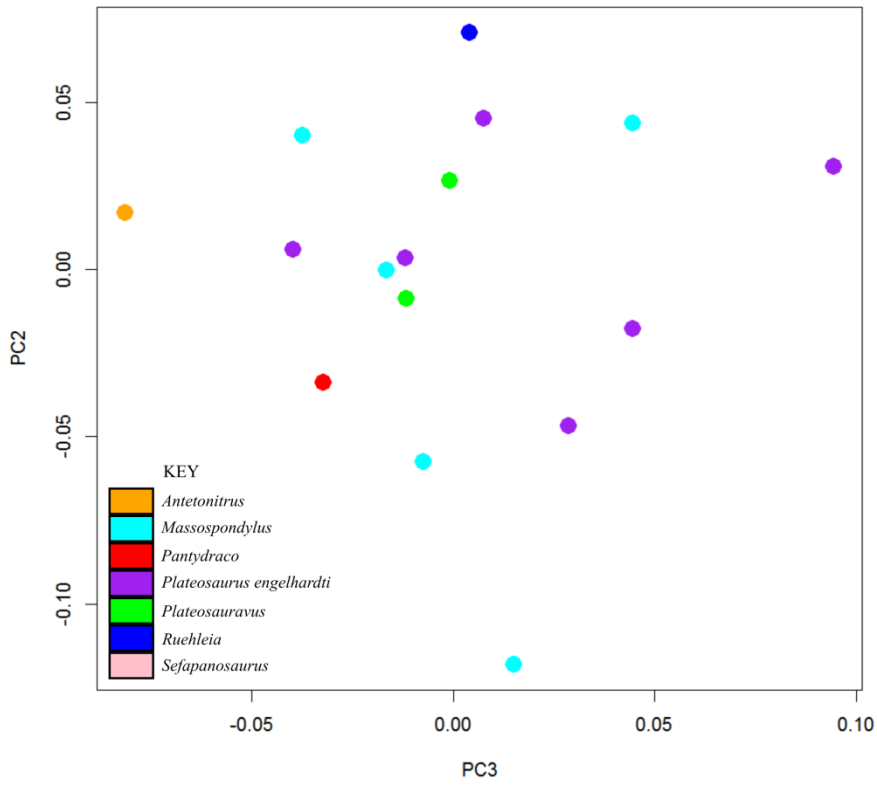

Figure (A1): PCA plot of PC2 vs PC3 of the proximal set of landmarks.

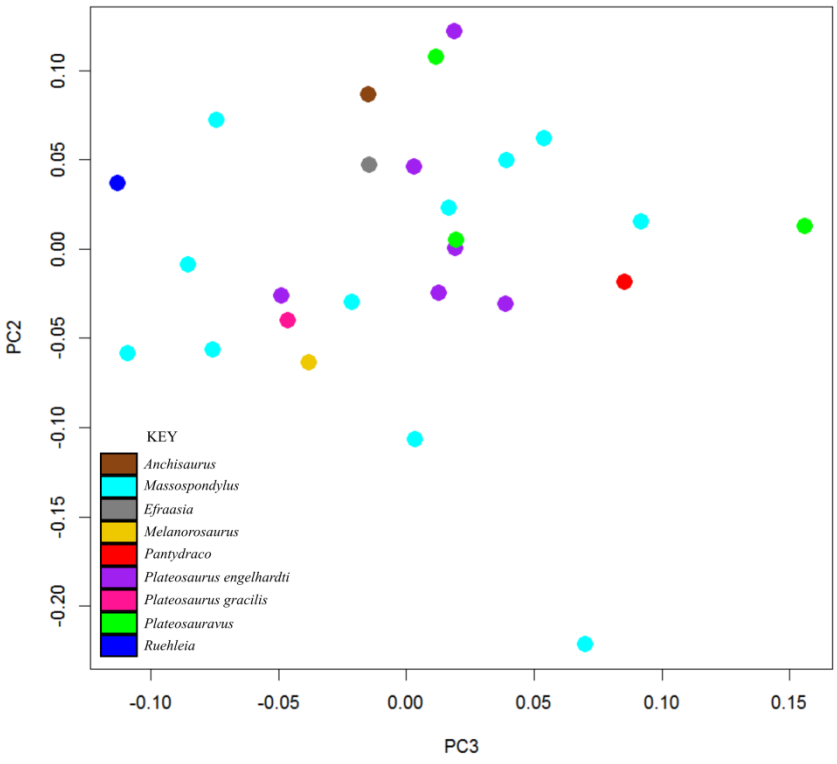

Figure (A2): PCA plot of PC2 vs PC3 of the distal set of landmarks

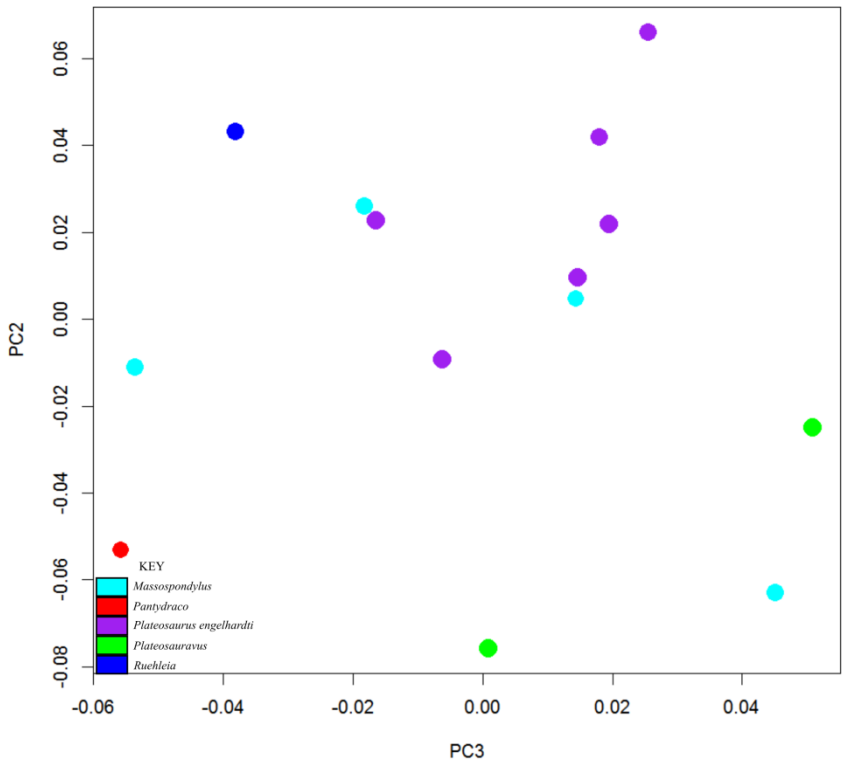

Figure (A3): PCA plot of PC2 vs PC3 of the complete set of landmarks.

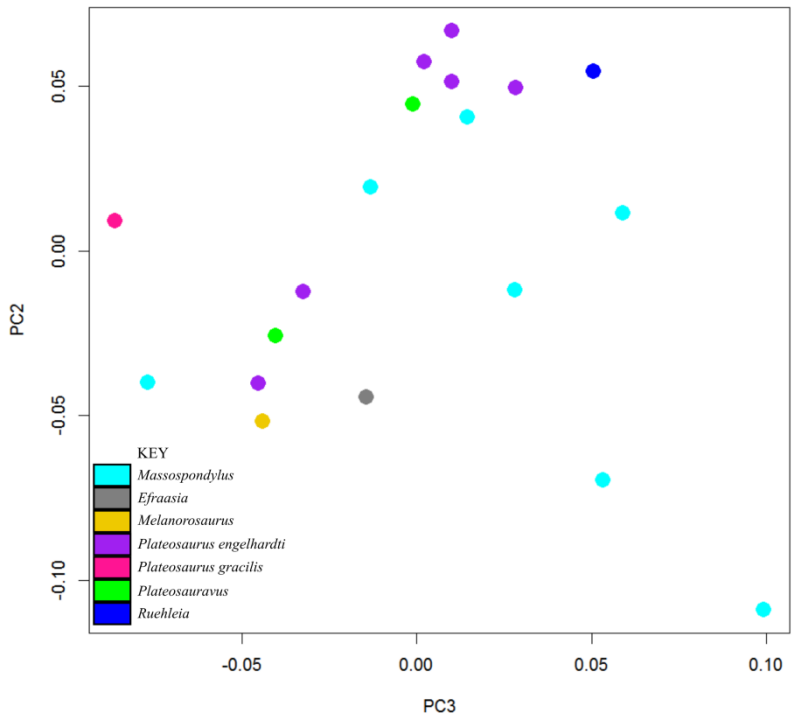

Figure (A4): PCA plot of PC2 vs PC3 of the olecranon and cuboid fossa of the distal humerus landmarks.

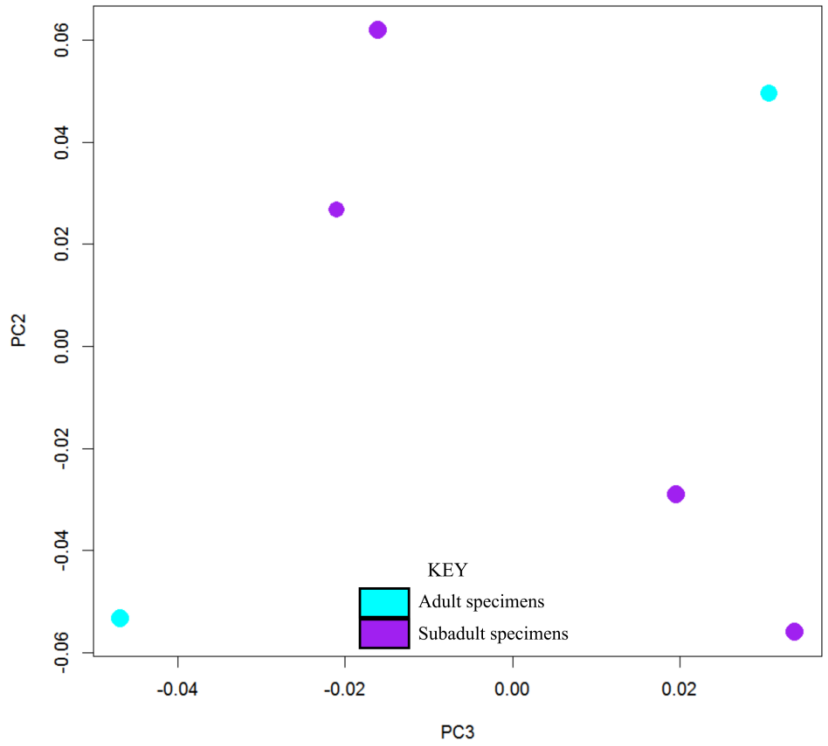

Figure (A5): PCA plot of PC2 vs PC3 of the proximal set of ontogeny landmarks.

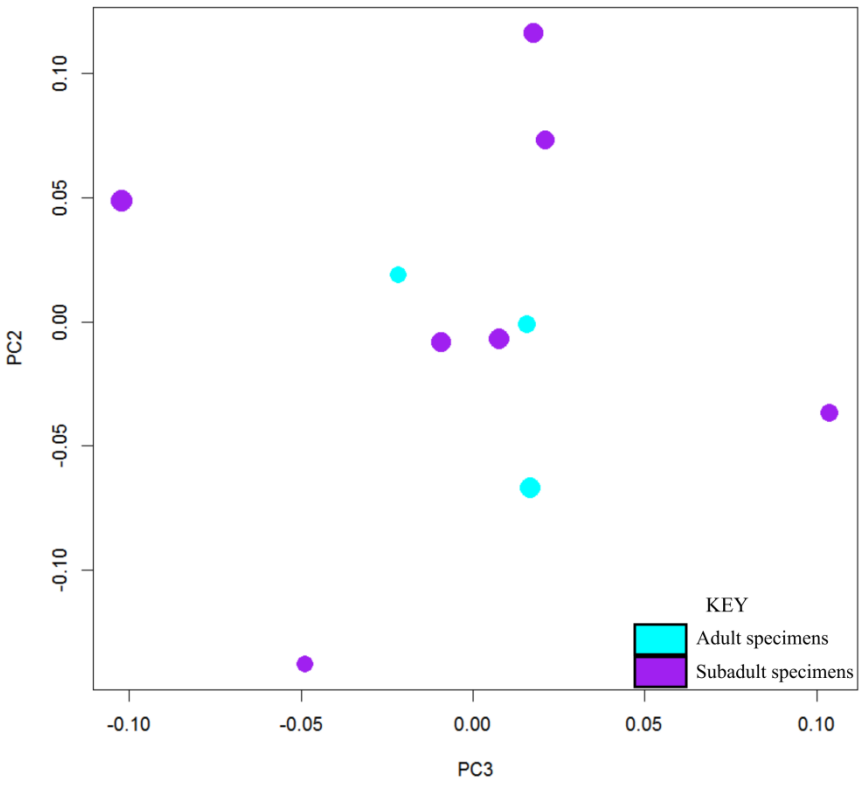

Figure (A6): PCA plot of PC2 vs PC3 of the distal set of ontogeny landmarks.

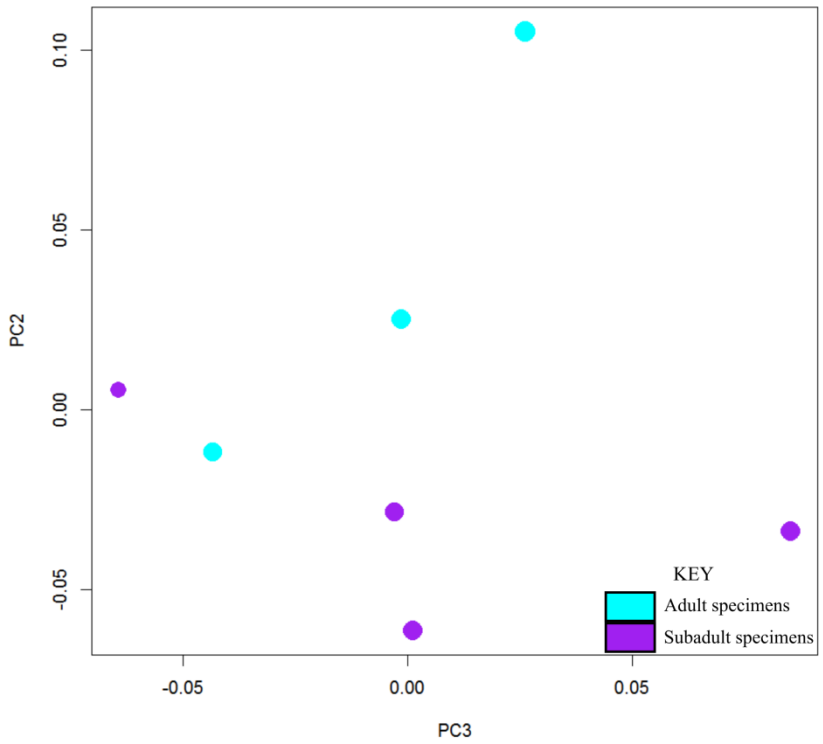

Figure (A7): PCA plot of PC2 vs PC3 of the fossae set of ontogeny landmarks.

Appendix 2 - Regression Plots and Data Tables

Proximal Landmark data

Table (A1): Regression data for proximal set of landmarks using centroid size vs Principal Components of interest.

	R^2	Adjusted R^2	P-value
PC1 vs Logged Centroid	0.329	0.282	0.02008
PC2 vs Logged Centroid	0.0272	-0.0423	0.5416
PC3 vs Logged Centroid	0.00577	-0.0652	0.7798

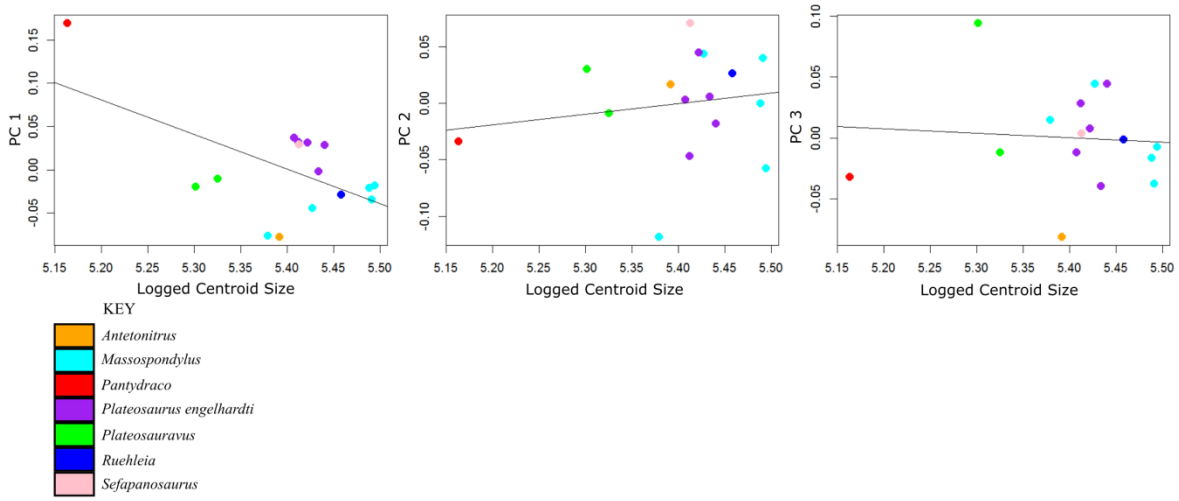

Figure (A8): Logged Centroid Size vs principal Components of interest for the proximal set of landmarks. From left to right; Logged Centroid Size vs PC1, Logged Centroid Size vs PC2, Logged Centroid Size vs PC3

Distal Landmark Data

Table (A2): Regression data for distal set of landmarks using centroid size vs Principal Components of interest.

	R^2	Adjusted R^2	P-value
PC1	0.159	0.124	0.04348
PC2	0.0313	-0.00903	0.387
PC3	0.000323	-0.0413	0.9305

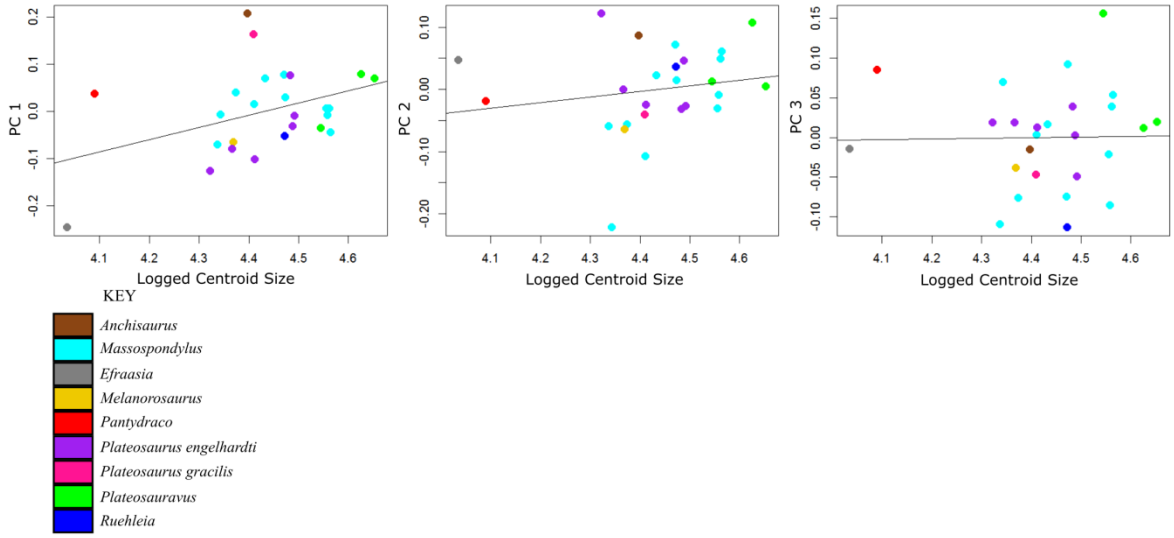

Figure (A9): Logged Centroid Size vs Principal Components of interest for the distal set of landmarks. From left to right; Logged Centroid Size vs PC1, Logged Centroid Size vs PC2, Logged Centroid Size vs PC3

Complete Landmark Data

Table (A3): Regression data for complete set of landmarks using centroid size vs Principal Components of interest.

	R^2	Adjusted R^2	P-value
PC1	0.0386	-0.0415	0.5007
PC2	0.00598	-0.0769	0.7927
PC3	0.122	0.0485	0.2215

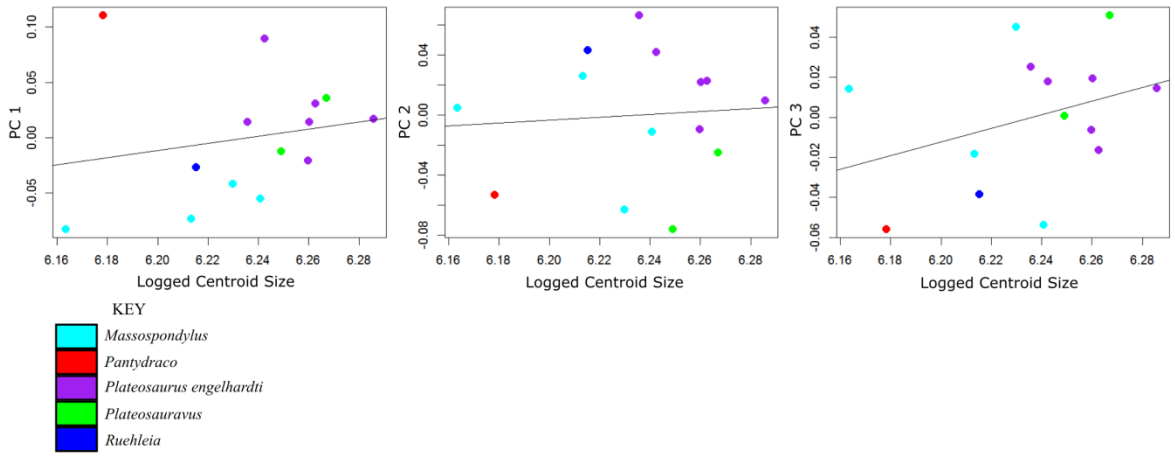

Figure (A10): Logged Centroid Size vs Principal Components of interest for the complete set of landmarks. From left to right; Logged Centroid Size vs PC1, Logged Centroid Size vs PC2, Logged Centroid Size vs PC3

Fossae Landmark Data

Table (A4): Regression data for Fossae set of landmarks using centroid size vs Principal Components of interest.

	R^2	Adjusted R^2	P-value
PC1	0.359	0.322	0.006662
PC2	0.13	0.0785	0.1298
PC3	0.0614	0.00622	0.3063

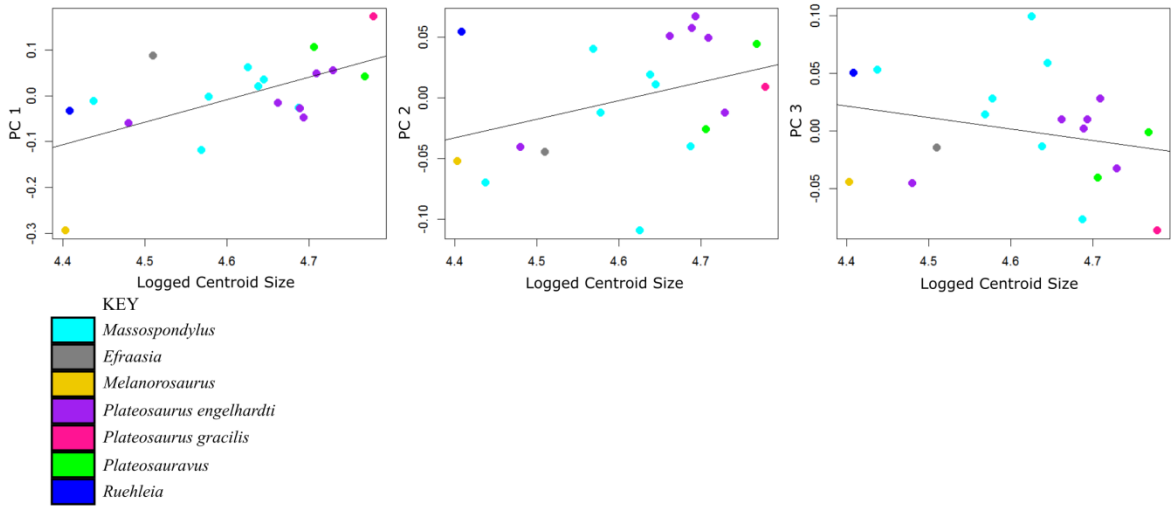

Figure (A11): Logged Centroid Size vs Principal Components of interest for the cuboid fossa and olecranon fossa set of landmarks. From left to right; Logged Centroid Size vs PC1, Logged Centroid Size vs PC2, Logged Centroid Size vs PC3

Proximal Ontogeny Landmark Data

Table (A5): Regression data for proximal ontogeny set of landmarks using centroid size vs Principal Components of interest.

	R^2	Adjusted R^2	P-value
PC1	0.241	0.0507	0.3233
PC2	0.421	0.276	0.1635
PC3	0.00838	-0.24	0.8631

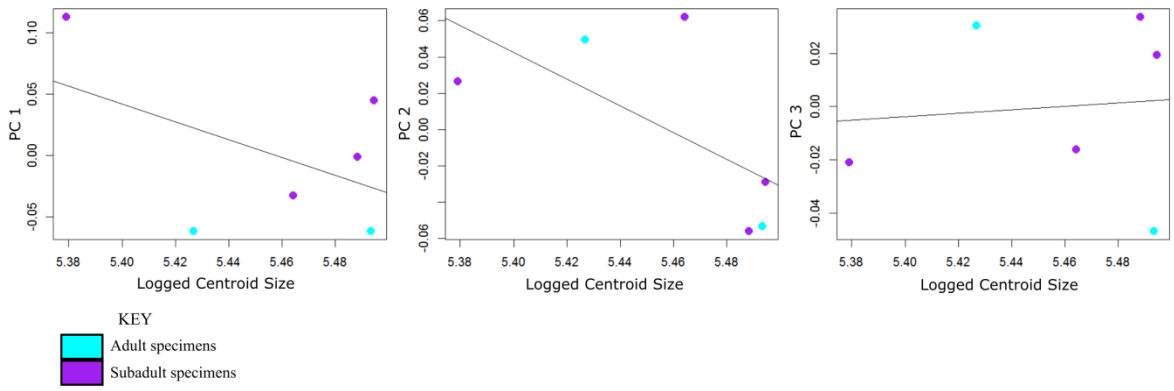

Figure (A12): Logged Centroid Size vs Principal Components of interest for the proximal ontogeny set of landmarks. From left to right; Logged Centroid Size vs PC1, Logged Centroid Size vs PC2, Logged Centroid Size vs PC3

Distal Ontogeny Landmark Data

Table (A6): Regression data for distal ontogeny set of landmarks using centroid size vs Principal Components of interest.

	R^2	Adjusted R^2	P-value
PC1	0.403	0.337	0.03573
PC2	0.112	0.0128	0.3155
PC3	0.0116	-0.0982	0.7523

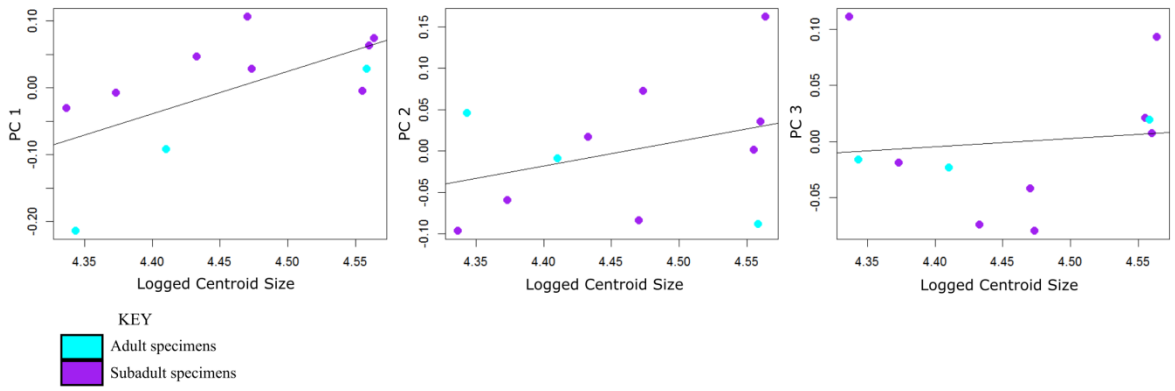

Figure (A13): Logged Centroid Size vs Principal Components of interest for the distal ontogeny set of landmarks. From left to right; Logged Centroid Size vs PC1, Logged Centroid Size vs PC2, Logged Centroid Size vs PC3

Fossae Ontogeny Data

Table (A7): Regression data for fossae ontogeny set of landmarks using centroid size vs Principal Components of interest.

	R^2	Adjusted R^2	P-value
PC1	0.00428	-0.195	0.8891
PC2	0.0506	-0.139	0.6277
PC3	0.547	0.457	0.05735

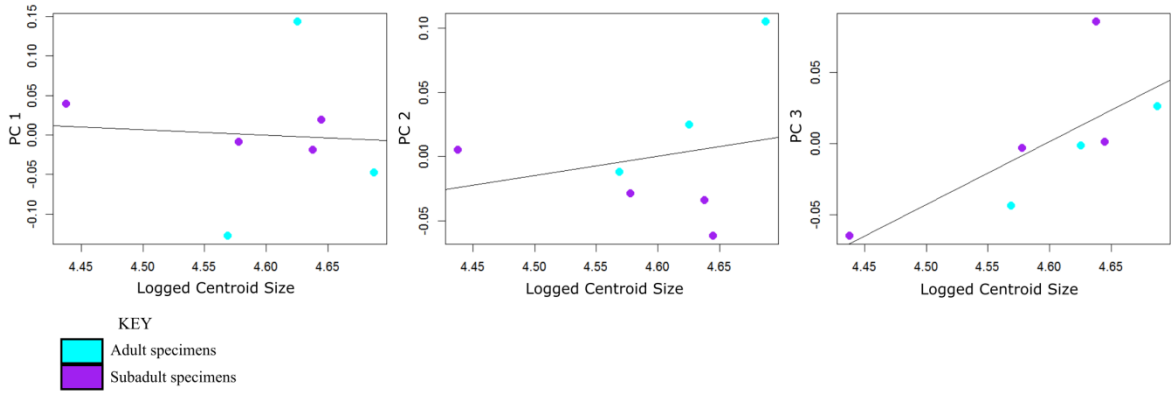

Figure (A14): Logged Centroid Size vs Principal Components of interest for the fossae ontogeny set of landmarks. From left to right; Logged Centroid Size vs PC1, Logged Centroid Size vs PC2, Logged Centroid Size vs PC3

Appendix 3 - R Scripts

The working R script as it was used to analyse the data for the PCAs can be found below. This was for the proximal set of data. For each set the working directory was changed and the script run.

```
require(Morpho)

require(abind)

#Set working directory for landmark files

	setwd("C:/Users/Casey/Documents/LANDMARK FILES/ProximalRerun")

		Bs_files<-list.files()

#Use scan() to read a landmark file from Amira, skipping 14 lines of other stuff

	Bs_landmarks<-list()


	for(i in 1:length(Bs_files)) {

		Bs_landmarks[[i]]<-scan(Bs_files[i],skip=14)

			Bs_landmarks[[i]]<-matrix(Bs_landmarks[[i]],ncol=3,byrow=TRUE)

				colnames(Bs_landmarks[[i]])<-c("x","y","z")

				rownames(Bs_landmarks[[i]])<-
paste(rep("lm",dim(Bs_landmarks[[i]])[1]),1:dim(Bs_landmarks[[i]])[1])

		}


		names(Bs_landmarks)<-unlist(strsplit(Bs_files,split=".landmarkAscii"))

#Look for discrepant landmarks by generating a table of discrepancy sizes

	landmarks_temp<-Bs_landmarks

		discrepancies<-list()


	for(j in 1:(length(landmarks_temp)/3)) {

		specimen_landmarks_temp<-abind(landmarks_temp[[j*3-2]],landmarks_temp[[j*3-
1]],landmarks_temp[[j*3]],along=3)

			dimnames(specimen_landmarks_temp)[[1]]<-
paste(rep("lm",dim(specimen_landmarks_temp)[1]),1:dim(specimen_landmarks_temp)[1])

			dimnames(specimen_landmarks_temp)[[2]]<-c("x","y","z")
```

```
dimnames(specimen_landmarks_temp)[[3]]<-c("1","2","3")

for(k in 1:dim(specimen_landmarks_temp)[1]) {

AA<-specimen_landmarks_temp[k,,]

BB<-c((sum((AA[,2]-AA[,3])^2)^0.5),(sum((AA[,1]-
AA[,3])^2)^0.5),(sum((AA[,1]-AA[,2])^2)^0.5))

if(k==1) {specimen_discrepancies<-BB}

if(k!=1) {specimen_discrepancies<-
rbind(specimen_discrepancies,BB)}

} ; rownames(specimen_discrepancies)<-
paste(rep("lm",dim(specimen_landmarks_temp)[1]),1:dim(specimen_landmarks_temp)[1]);
colnames(specimen_discrepancies)<-c("2 vs 3","1 vs 3","1 vs 2")

discrepancies[[j]]<-specimen_discrepancies

}; names(discrepancies)<-unlist(strsplit(names(landmarks_temp),split="
lm"))[seq(1,length(landmarks_temp)*2,by=6)]

#Plot a histogram showing all discrepancy sizes for all attempts at all landmarks

dev.new(width=8,height=5)

hist(do.call(rbind,discrepancies),breaks=30)


abline(v=quantile(do.call(rbind,discrepancies),probs=c(0.90,0.95)),lty=2,lwd=2,col="grey")

#Plot a histogram showing all discrepancy sizes for one specimen - X chooses the specimen to use

X=1

for(X in 1:length(discrepancies)) {

dev.new(width=8,height=5)

hist(discrepancies[[X]],breaks=30,main=paste(c("Landmark attempt discrepancy
sizes for
",names(discrepancies)[X]),collapse=""),xlim=c(0,max(do.call(rbind,discrepancies),na.rm=TRUE)))


abline(v=quantile(do.call(rbind,discrepancies),probs=c(0.90,0.95)),lty=2,lwd=2,col="grey")

}

#Choose a threshold discrepancy size to reject attempts at landmarking

threshold=1
```

```
	threshold=quantile(do.call(rbind,discrepancies),probs=c(0.925))


	for(j in 1:length(discrepancies)) {

			find_discrepancies<-discrepancies[[j]]>threshold

#Find the discrepant landmark attempts ("bad_attempts") and replace them with "NA" in landmarks_temp

		bad_attempts<-c(1)

	if(sum(apply(find_discrepancies,1,sum)==2)==1) {bad_attempts<-which(!find_discrepancies[apply(find_discrepancies,1,sum)==2,])}

	if(sum(apply(find_discrepancies,1,sum)==2)>1) {bad_attempts<-apply(!find_discrepancies[apply(find_discrepancies,1,sum)==2,],1,which)}


	for(l in 1:length(bad_attempts)) {

		if(sum(apply(find_discrepancies,1,sum)==2)>0) {

			landmarks_temp[[j*3-3+bad_attempts[l]]][rownames(find_discrepancies)[apply(find_discrepancies,1,sum)==2][l],]<-NA

		}

			}


				}

#At this point it is advisable to inspect the object "landmarks_temp"

	landmarks_temp

#Format the data for relative warps using mean positions of each landmark across non-discrepant attempts

	for(j in 1:(length(landmarks_temp)/3))	{

		specimen_landmarks_temp<-abind(landmarks_temp[[j*3-2]],landmarks_temp[[j*3-1]],landmarks_temp[[j*3]],along=3)

			if(j==1) {mean_landmarks<-apply(specimen_landmarks_temp,c(1,2),mean,na.rm=TRUE)}

			if(j>1) {mean_landmarks<-abind(mean_landmarks,apply(specimen_landmarks_temp,c(1,2),mean,na.rm=TRUE),along=3)}
```

```
        }; dimnames(mean_landmarks)[[3]]<-unlist(strsplit(names(landmarks_temp),split="
lm"))[seq(1,length(landmarks_temp)*2,by=6)]

#Do relative warps analysis using Morpho

        results<-relWarps(mean_landmarks, alpha=0)

        sizes<-apply(mean_landmarks,3,cSize)

#Plot x and y dimensions of       mean shape

        plot(results$mshape[,1],results$mshape[,2])

        plot(results$mshape[,2],results$mshape[,3])

        plot(results$mshape[,1],results$mshape[,3])

#Plot PC1 vs PC2 and PC2 vs PC3

sizes_sorted<-sort(sizes,decreasing=FALSE)

size_points<-(sizes/sizes_sorted[1]*2)

dev.new(width=10,height=5)

        close.screen(all.screens=TRUE)

                split.screen(c(1,2))

                        screen(1)


        plot(results$bescores[,1],results$bescores[,2],xlab="PC1",ylab="PC2",main="PC2 vs
PC1",cex=2,col=c("orange", "cyan", "cyan", "cyan", "cyan", "cyan", "red", "purple", "purple",
"purple", "purple", "purple", "green", "green", "blue", "pink"), pch=16)


        text(results$bescores[,1],results$bescores[,2],rownames(results$bescores),cex=1,pos=c(4, 2,
4, 1, 2, 4, 2, 2), offset=1)

                                        #legend("topleft", legend=c("juvenile", "subadult", "adult"),
col=c("green", "purple", "orange"), pch=2, lwd=3)


                        screen(2)


        plot(results$bescores[,3],results$bescores[,2],xlab="PC3",ylab="PC2",main="PC2 vs
PC3",cex=2, col=c("orange", "cyan", "cyan", "cyan", "cyan", "cyan", "red", "purple", "purple",
"purple", "purple", "purple", "purple", "purple", "green", "green", "blue", "pink"), pch=16)
```

```
text(results$bescores[,3],results$bescores[,2],rownames(results$bescores),cex=1,pos=c(4, 2, 4, 1, 4, 4, 2, 4), offset=1)

#R2 and Pvalues

reg<-lm(results$bescores[,K]~log(sizes, base = exp(1)))

pvals<-summary(reg)$coefficients[2,4]

slopes<-summary(reg)$coefficients[1,4]

R2s<-summary(reg)$adj.r.squared

#Plot centroid size vs Pcs 1 to 6

dev.new(width=24,height=20)

close.screen(all.screens=TRUE)

split.screen(c(2,3))

for(K in 1:6) {

screen(K)

par(mar=c(2,2,2,2))

plot(log(sizes, base = exp(1)),results$bescores[,K], col=c("orange", "cyan", "cyan", "cyan", "cyan", "cyan", "red", "purple", "purple", "purple", "purple", "purple", "green", "green", "blue", "pink"), pch=16, cex=1.5)

text(log(sizes, base = exp(1)), results$bescores[,K], labels=rownames(results$bescores), pos=c(4, 2, 2, 4, 4, 4, 4, 4), cex=0.8)

reg<-lm(results$bescores[,K]~log(sizes, base = exp(1)))

abline(reg, lwd=0.5)

#R2 and Pvalues

pvals[K]<-summary(reg)$coefficients[2,4]

slopes[K]<-summary(reg)$coefficients[1,4]

R2s[K]<-summary(reg)$adj.r.squared

}

#This tells you the variances explained by each axis

results$Var

results$Var[,2]
```

The working R script as it was used to analyse the data for the Goodall's F-tests can be found below. For each set the working directory was changed and the script run.

```
require(Morpho)

require(abind)

require(Shapes)

#Set working directory for landmark files

        setwd("C:/Users/Casey/Documents/LANDMARK FILES/Ontogeny LM R/Proximal")

                Bs_files<-list.files()



#Use scan() to read a landmark file from Amira, skipping 14 lines of other stuff

        Bs_landmarks<-list()


        for(i in 1:length(Bs_files)) {

                Bs_landmarks[[i]]<-scan(Bs_files[i],skip=14)

                        Bs_landmarks[[i]]<-matrix(Bs_landmarks[[i]],ncol=3,byrow=TRUE)

                                colnames(Bs_landmarks[[i]])<-c("x","y","z")

                                rownames(Bs_landmarks[[i]])<-
paste(rep("lm",dim(Bs_landmarks[[i]])[1]),1:dim(Bs_landmarks[[i]])[1])

                }


                names(Bs_landmarks)<-unlist(strsplit(Bs_files,split=".landmarkAscii"))



#Look for discrepant landmarks by generating a table of discrepancy sizes

        landmarks_temp<-Bs_landmarks

                discrepancies<-list()


        for(j in 1:(length(landmarks_temp)/3)) {
```

```
        specimen_landmarks_temp<-abind(landmarks_temp[[j*3-2]],landmarks_temp[[j*3-
1]],landmarks_temp[[j*3]],along=3)

            dimnames(specimen_landmarks_temp)[[1]]<-
paste(rep("lm",dim(specimen_landmarks_temp)[1]),1:dim(specimen_landmarks_temp)[1])

            dimnames(specimen_landmarks_temp)[[2]]<-c("x","y","z")

            dimnames(specimen_landmarks_temp)[[3]]<-c("1","2","3")


    for(k in 1:dim(specimen_landmarks_temp)[1]) {

        AA<-specimen_landmarks_temp[k,,]

            BB<-c((sum((AA[,2]-AA[,3])^2)^0.5),(sum((AA[,1]-
AA[,3])^2)^0.5),(sum((AA[,1]-AA[,2])^2)^0.5))

                if(k==1) {specimen_discrepancies<-BB}

                if(k!=1) {specimen_discrepancies<-
rbind(specimen_discrepancies,BB)}

                } ; rownames(specimen_discrepancies)<-
paste(rep("lm",dim(specimen_landmarks_temp)[1]),1:dim(specimen_landmarks_temp)[1]);
colnames(specimen_discrepancies)<-c("2 vs 3","1 vs 3","1 vs 2")

        discrepancies[[j]]<-specimen_discrepancies

    }; names(discrepancies)<-unlist(strsplit(names(landmarks_temp),split="
lm"))[seq(1,length(landmarks_temp)*2,by=6)]




#Choose a threshold discrepancy size to reject attempts at landmarking

    threshold=1

    threshold=quantile(do.call(rbind,discrepancies),probs=c(0.925))


    for(j in 1:length(discrepancies)) {

            find_discrepancies<-discrepancies[[j]]>threshold



#Find the discrepant landmark attempts ("bad_attempts") and replace them with "NA" in
landmarks_temp
```

```
		bad_attempts<-c(1)

	if(sum(apply(find_discrepancies,1,sum)==2)==1) {bad_attempts<-
which(!find_discrepancies[apply(find_discrepancies,1,sum)==2,])}

	if(sum(apply(find_discrepancies,1,sum)==2)>1) {bad_attempts<-
apply(!find_discrepancies[apply(find_discrepancies,1,sum)==2,],1,which)}



	for(l in 1:length(bad_attempts)) {

		if(sum(apply(find_discrepancies,1,sum)==2)>0) {

			landmarks_temp[[j*3-
3+bad_attempts[l]]][rownames(find_discrepancies)[apply(find_discrepancies,1,sum)==2][l],]<-NA

		}

			}


				}

#At this point it is advisable to inspect the object "landmarks_temp"

	landmarks_temp



#Format the data for relative warps using mean positions of each landmark across non-discrepant
attempts

	for(j in 1:(length(landmarks_temp)/3))	{

		specimen_landmarks_temp<-abind(landmarks_temp[[j*3-2]],landmarks_temp[[j*3-
1]],landmarks_temp[[j*3]],along=3)

			if(j==1) {mean_landmarks<-
apply(specimen_landmarks_temp,c(1,2),mean,na.rm=TRUE)}

			if(j>1) {mean_landmarks<-
abind(mean_landmarks,apply(specimen_landmarks_temp,c(1,2),mean,na.rm=TRUE),along=3)}

		}; dimnames(mean_landmarks)[[3]]<-unlist(strsplit(names(landmarks_temp),split="
lm"))[seq(1,length(landmarks_temp),by=3)]



adultPos<-c(1,6)
```

```
adultLandmarks<-mean_landmarks[ , ,adultPos]

subadultLandmarks<-mean_landmarks[ , ,-adultPos]


testmeanshapes(adultLandmarks, subadultLandmarks, resamples = 1000, replace = FALSE, scale =
TRUE)
```

Appendix 4 - Excluded Specimens from Landmark Set and Torsion Measurements

Table (A8): Specimens in the proximal set missing landmarks and which numbers are missing and were excluded from the set.

Species	Specimen Number	Missing Landmark Number
Efraasia	SMNS 12668	7, 8
Massospondylus	BP/1/4732	3, 5
Massospondylus	BP/1/5001	7, 8
Melanorosaurus	SAM PK 3450	1
Melanorosaurus	SAM PK 3532	7, 8
Plateosaurus gracilis	SMNS 12354	7
Plateosauravus	BPI/1/7358	9, 10

Table (A9): Specimens in the distal set missing landmarks and which numbers are missing were excluded from the set.

Species	Specimen Number	Missing Landmark Number
Antetonitrus	BPI/1/4952	1, 5, 6, 7, 8
Massospondylus	BP/1/6125	7

Table (A10): Specimens missing landmarks and which numbers are missing and were excluded from the set.

Species	Specimen Number	Missing Landmark Number
Antetonitrus	BPI/1/4952	15, 19, 20, 21, 22
Efraasia	SMNS 12668	7, 8
Massospondylus	BP/1/4732	3, 5
Massospondylus	BP/1/5001	7, 8
Melanorosaurus	SAM PK 3532	7, 8

Plateosaurus gracilis	SMNS 12354	7
Plateosauravus	BPI/1/7358	9, 10

Table (A11): Measured angles of humeral torsion for key specimens.

Species	**Specimen Number**	**Angle of Torsion**
Antetonitrus	BPI/1/4952	37°
Efraasia	SMNS 12668	53°
Massospondylus	BP/1/4934 (Big Momma)	32°
	BP/1/4998a	21.5 °(This specimen is distorted)
	BP/1/4998b	28°
	BP/1/5000	28.3°
Melanorosaurus	SAM PK 3532	30.5°
Pantydraco	BMNH 19 7	12°
Plateosaurus engelhardti	MBR 4430 163	20.2°
	SMNS 12949	31.5°
	SMNS 20664	44.1°
	SMNS 53537	20.1°
	SMNS 91296	30°
	SMNS 91310	28.3°
Plateosauravus	SAM PK 3342	27.8°
	SAM PK 3350	7.1°

Appendix 5 - Additional PCAs of the proximal and distal Sets where juveniles were excluded

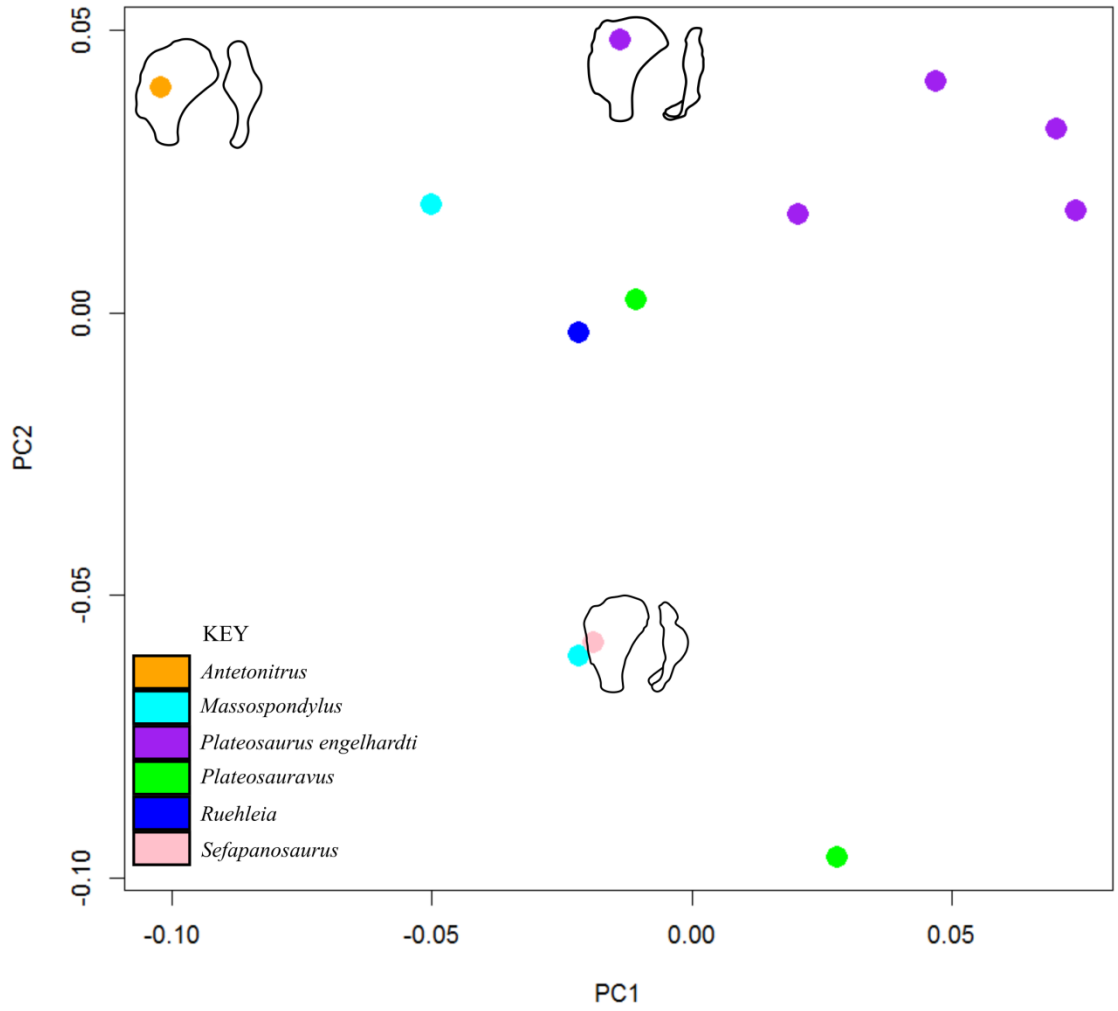

Figure (A15): PCA plot of PC1 vs PC2 of the proximal set of landmarks where all juvenile specimens were removed with colour key to indicate species and line drawings indicate the most extreme examples of morphology. PC1 shows (24.33% of variance) describes a change from more domed humeral heads with symmetrical expansions on to the lateral and medial humerus to less domed heads with a greater lateral expansion and more prominent deltopectoral crests. PC2 (20.67% of variance) seems to be revealing lots of intraspecific variation.

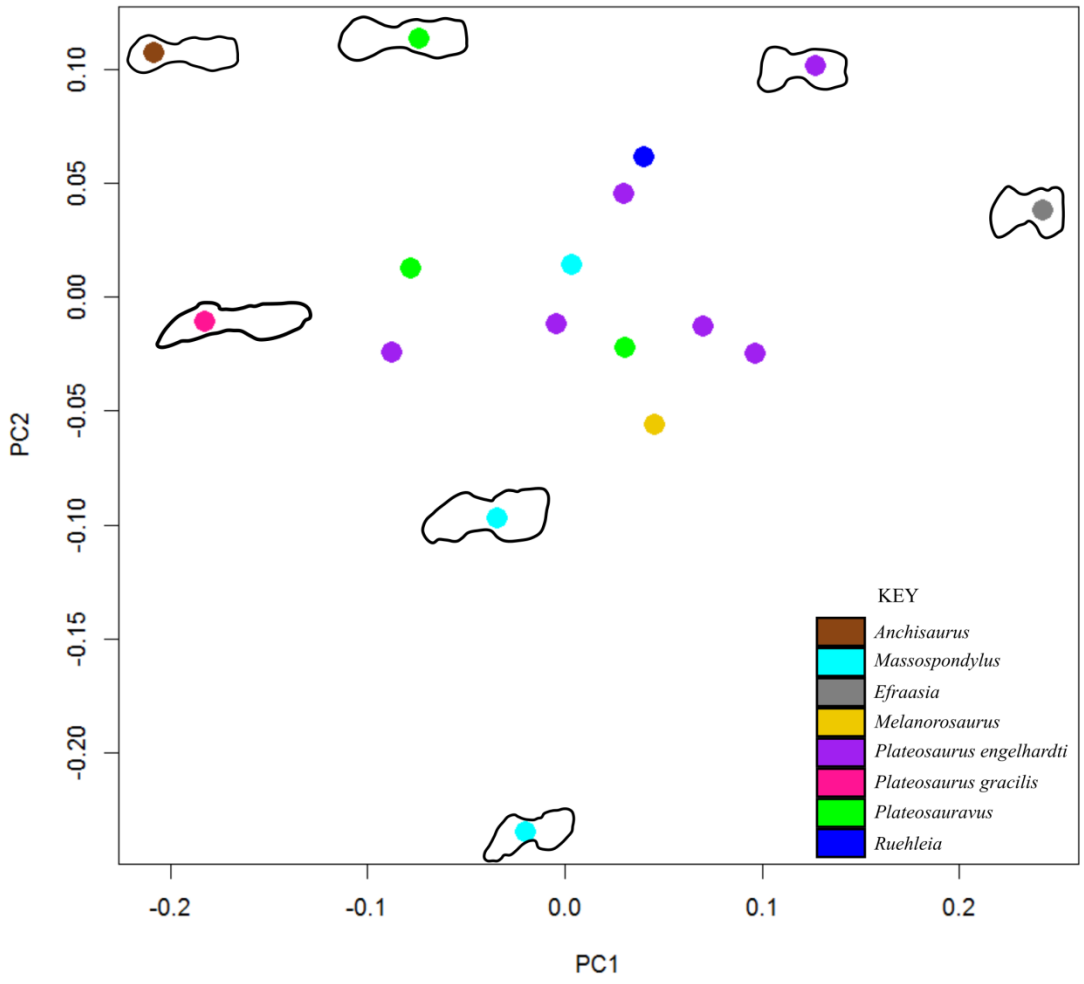

Figure (A16): PCA plot of PC1 vs PC2 of the distal set of landmarks where all juvenile specimens were removed with colour key to indicate species and line drawings indicate the most extreme examples of morphology. PC1 (37.45% of variance) describes the change in the deflection of the radial condyle as well as condyle symmetry while PC2 (21.91% of variance) describes the distance between the condyles.

6.References

Apaldetti, C., Martinez, R. N., Alcober, O. A., & Pol, D. (2011). A new basal sauropodomorph (Dinosauria: Saurischia) from Quebrada del Barro Formation (Marayes-El Carrizal Basin), northwestern Argentina. *PLoS One*, *6*(11), e26964.

Barrett, P. M. (2004). Sauropodomorph dinosaur diversity in the upper Elliot Formation (*Massospondylus* range zone: Lower Jurassic) of South Africa: research letter. *South African Journal of Science*, *100*(9-10), 501-503.

Barrett, P. M. (2009). A new basal sauropodomorph dinosaur from the upper Elliot Formation (Lower Jurassic) of South Africa. *Journal of Vertebrate Paleontology*, *29*(4), 1032-1045.

Barrett, P. M., McGowan, A. J., & Page, V. (2009). Dinosaur diversity and the rock record. *Proceedings of the Royal Society of London B: Biological Sciences*, *276*(1667), 2667-2674.

Barrett, P. M., Butler, R. J., & Nesbitt, S. J. (2010). The roles of herbivory and omnivory in early dinosaur evolution. *Earth and Environmental Science Transactions of the Royal Society of Edinburgh*, *101*(3-4), 383-396.

Benson, R. B., Campione, N. E., Carrano, M. T., Mannion, P. D., Sullivan, C., Upchurch, P., & Evans, D. C. (2014). Rates of dinosaur body mass evolution indicate 170 million years of sustained ecological innovation on the avian stem lineage. *PLoS Biol*, *12*(5), e1001853.

Biewener, A. A. (1989). Scaling body support in mammals: limb posture and muscle mechanics. *Science*, *245*(4913), 45-48.

Bonnan, M. F. (2003). The evolution of manus shape in sauropod dinosaurs: implications for functional morphology, forelimb orientation, and phylogeny. *Journal of Vertebrate Paleontology*, *23*(3), 595-613.

Bonnan, M. F. (2004). Morphometric analysis of humerus and femur shape in Morrison sauropods: implications for functional morphology and paleobiology. *Paleobiology*, *30*(3), 444-470.

Bonnan, M. F. (2007). Linear and geometric morphometric analysis of long bone scaling patterns in Jurassic neosauropod dinosaurs: their functional and paleobiological implications. *The Anatomical Record*, *290*(9), 1089-1111.

Bonnan, M. F., & Senter, P. (2007). Were the basal sauropodomorph dinosaurs *Plateosaurus* and *Massospondylus* habitual quadrupeds?. *Evolution and palaeobiology of early sauropodomorph dinosaurs*, (77), 139-155.

Bonnan, M. F., & Yates, A. M. (2007). A new description of the forelimb of the basal sauropodomorph *Melanorosaurus*: implications for the evolution of pronation, manus shape and quadrupedalism in sauropod dinosaurs. *Evolution and palaeobiology of early sauropodomorph dinosaurs*, (77), 157-168.

Bonnan, M. F., Wilhite, D. R., Masters, S. L., Yates, A. M., Gardner, C. K., & Aguiar, A. (2013). What lies beneath: sub-articular long bone shape scaling in eutherian mammals and saurischian dinosaurs suggests different locomotor adaptations for gigantism. *PloS one*, *8*(10), e75216.

Bookstein, F. L. (1997). *Morphometric tools for landmark data: geometry and biology*. Cambridge University Press.

Breithaupt, B. H., Matthews, N. A., & Noble, T. A. (2004). An integrated approach to three-dimensional data collection at dinosaur tracksites in the Rocky Mountain West. *Ichnos*, *11*(1-2), 11-26.

Burch, S. H. (2014). Complete forelimb myology of the basal theropod dinosaur *Tawa hallae* based on a novel robust muscle reconstruction method. *Journal of anatomy*, *225*(3), 271-297.

Carrano, M. T. (2005). The evolution of sauropod locomotion. *The sauropods: evolution and paleobiology. University of California Press, Berkeley*, 229-249.

Chinsamy, A (1993). Bone histology and growth trajectory of the prosauropod dinosaur *Massospondylus* carinatus Owen. *Modern Geology*, *18*(3), 319-329.

Dilkes, D. W. (2001). An ontogenetic perspective on locomotion in the Late Cretaceous dinosaur *Maiasaura peeblesorum* (Ornithischia: Hadrosauridae). *Canadian Journal of Earth Sciences*, *38*(8), 1205-1227.

Dryden, I. L. (2017). shapes: Statistical Shape Analysis. R package version 1.2.0. https://CRAN.R-project.org/package=shapes

de Fabrègues, C. P., Allain, R., & Barriel, V. (2015). Root causes of phylogenetic incongruence observed within basal sauropodomorph interrelationships. *Zoological Journal of the Linnean Society*, *175*(3), 569-586.

de Fabrègues, C. P., & Allain, R. (2016). New material and revision of *Melanorosaurus thabanensis*, a basal sauropodomorph from the Upper Triassic of Lesotho. *PeerJ*, *4*, e1639.

Falkingham, P. L. (2012). Acquisition of high resolution three-dimensional models using free, open-source, photogrammetric software. *Palaeontologia electronica*, *15*(1), 15.

Fujiwara, S. I., Taru, H., & Suzuki, D. (2010). Shape of articular surface of crocodilian (Archosauria) elbow joints and its relevance to sauropsids. *Journal of Morphology*, *271*(7), 883-896.

Galton, P. M. (2001). Prosauropod dinosaurs from the Upper Triassic of Germany. *Actas de las I Jornadas Internacionales sobre Paleontologia de Dinosaurios y su Entorno, Junta de Castilla y León, Salas de los Infantes, Burgos, España*, 25-92.

Galton, P. M., & Upchurch, P. (2004). Prosauropoda. University of California Press.

Galton, P. M., & Van Heerden, J. (1985). Partial hindlimb of *Blikanasaurus cromptoni* n. gen. and n. sp., representing a new family of prosauropod dinosaurs from the Upper Triassic of South Africa. *Geobios*, *18*(4), 509-516.

Galton, P. M., Yates, A. M., & Kermack, D. (2007). *Pantydraco* n. gen. for *Thecodontosaurus caducus* Yates, 2003, a basal sauropodomorph dinosaur from the Upper Triassic or Lower Jurassic of South Wales, UK. *Neues Jahrbuch für Geologie und Paläontologie-Abhandlungen*, *243*(1), 119-125.

Hammer, Ø. (2002). Morphometrics-brief notes. *Paläontologisches Institut und Museum, Zürich*

Heinrich, R. E., Ruff, C. B., & Weishampel, D. B. (1993). Femoral ontogeny and locomotor biomechanics of *Dryosaurus lettowvorbecki* (Dinosauria, Iguanodontia). *Zoological Journal of the Linnean Society*, *108*(2), 179-196.

Hildebrand, M., & Goslow, G. (2001). Analysis of Vertebrate Structure. 5th ed. *Inc. New York*.

Hutchinson, J. R. (2006). The evolution of locomotion in archosaurs. *Comptes Rendus Palevol*, *5*(3), 519-530.

Hutchinson, J. R., & Garcia, M. (2002). *Tyrannosaurus* was not a fast runner. *Nature*, *415*(6875), 1018-1021.

Iqbal, S. (2015). *The functional morphology and internal structure of the forelimb of the Early Triassic non-mammaliaform cynodont Thrinaxodon liorhinus* (Masters dissertation University of the Witwatersrand).

Kermack, D. (1984). New prosauropod material from South Wales. *Zoological Journal of the Linnean Society*, *82*(1-2), 101-117.

Kilbourne, B. M., & Hoffman, L. C. (2013). Scale effects between body size and limb design in quadrupedal mammals. *PLoS One, 8(11)*, e78392.

Kitching, J. W., & Raath, M. A. (1984). Fossils from the Elliot and Clarens Formations (Karoo Sequence) of the northeastern Cape, Orange Free State and Lesotho, and a suggested biozonation based on tetrapods. *Palaeontologia Africana*, *25*, 111–125

Klein, N., & Sander, P. M. (2007). Bone histology and growth of the prosauropod dinosaur *Plateosaurus engelhardti* von Meyer, 1837 from the Norian bonebeds of Trossingen (Germany) and Frick (Switzerland). *Special Papers in Palaeontology*, *77*, 169.

Kruger, A., Randolph-Quinney, P., & Elliott, M. (2016). Multimodal spatial mapping and visualisation of Dinaledi Chamber and Rising Star Cave. *South African Journal of Science*, *112*(5-6), 1-11.

Kundrát, M., Cruickshank, A. R., Manning, T. W., & Nudds, J. (2008). Embryos of therizinosauroid theropods from the Upper Cretaceous of China: diagnosis and analysis of ossification patterns. *Acta Zoologica*, *89*(3), 231-251.

Landsmeer, J. M. (1983). The mechanism of forearm rotation in *Varanus exanthematicus*. *Journal of Morphology*, *175*(2), 119-130.

Langer, M. C. (2003). The pelvic and hind limb anatomy of the stem-sauropodomorph *Saturnalia tupiniquim* (Late Triassic, Brazil). *PaleoBios 23(2*), 1–30

Langer, M. C., Abdala, F., Richter, M., & Benton, M. J. (1999). A sauropodomorph dinosaur from the Upper Triassic (Carman) of southern Brazil. *Comptes Rendus de l'Académie des Sciences-Series IIA-Earth and Planetary Science*, *329*(7), 511-517.

Langer, M. C., Franca, M. A., & Gabriel, S. (2007). The pectoral girdle and forelimb anatomy of the stem-sauropodomorph *Saturnalia tupiniquim* (Upper Triassic, Brazil). *Special Papers in Palaeontology*, *77*, 113

Larson, S. G. (1995). New characters for the functional interpretation of primate scapulae and proximal humeri. *American Journal of Physical Anthropology*, *98*(1), 13-35.

Livingston, V. J., Bonnan, M. F., Elsey, R. M., Sandrik, J. L., & Wilhite, D. (2009). Differential limb scaling in the American alligator (*Alligator mississippiensis*) and its implications for archosaur locomotor evolution. *The Anatomical Record*, *292*(6), 787-797.

Maidment, S. C., & Barrett, P. M. (2011). The locomotor musculature of basal ornithischian dinosaurs. *Journal of Vertebrate Paleontology*, *31*(6), 1265-1291.

Maidment, S. C., & Barrett, P. M. (2012). Does morphological convergence imply functional similarity? A test using the evolution of quadrupedalism in ornithischian

dinosaurs. *Proceedings of the Royal Society of London B: Biological Sciences*, *279*(1743), 3765-3771.

Mallison, H. (2010a). The digital *Plateosaurus* I: body mass, mass distribution, and posture assessed using CAD and CAE on a digitally mounted complete skeleton. *Palaeontologia Electronica*, *13*(13.2).

Mallison, H. (2010b). The digital *Plateosaurus* II: an assessment of the range of motion of the limbs and vertebral column and of previous reconstructions using a digital skeletal mount. *Acta Palaeontologica Polonica*, *55*(3), 433-458.

Mallison, H., & Wings, O. (2014). Photogrammetry in paleontology—a practical guide. *Journal of Paleontological Techniques*, *12*, 1-31.

Mannion, P. D. (2009). Review and analysis of African sauropodomorph dinosaur diversity. *Palaeontologia Africana*, *44*, 108-111.

Marsh, A. D. (2013). The osteology of *Sarahsaurus aurifontanalis* and geochemical observations of the dinosaurs from the type quarry of *Sarahsaurus* (Kayenta Formation), Coconino County, Arizona.

Martinez, R. N., & Alcober, O. A. (2009). A basal sauropodomorph (Dinosauria: Saurischia) from the Ischigualasto Formation (Triassic, Carnian) and the early evolution of Sauropodomorpha. *PLoS One*, *4*(2), e4397.

Mazzetta, G. V., Christiansen, P., & Fariña, R. A. (2004). Giants and bizarres: body size of some southern South American Cretaceous dinosaurs. *Historical Biology*, *16*(2-4), 71-83.

McPhee, B. W., Yates, A. M., Choiniere, J. N., & Abdala, F. (2014). The complete anatomy and phylogenetic relationships of *Antetonitrus ingenipes* (Sauropodiformes, Dinosauria): implications for the origins of Sauropoda. *Zoological Journal of the Linnean Society*, *171*(1), 151-205.

McPhee, B. W., Bonnan, M. F., Yates, A. M., Neveling, J., & Choiniere, J. N. (2015). A new basal sauropod from the pre-Toarcian Jurassic of South Africa: evidence of niche-partitioning at the sauropodomorph–sauropod boundary?. *Scientific reports*, *5*.

Meers, M. B. (2003). Crocodylian forelimb musculature and its relevance to Archosauria. *The Anatomical Record Part A: Discoveries in Molecular, Cellular, and Evolutionary Biology*, *274*(2), 891-916.

Meijer, K. (1998). *Muscle mechanics; the effect of stretch and shortening on skeletal muscle force*. Universiteit Twente.

Meyer, C. A., & Thüring, B. (2003). Dinosaurs of Switzerland. *Comptes Rendus Palevol*, *2*(1), 103-117.

Norman, D. B. (1980). On the ornithischian dinosaur Iguanodon bernissartensis from the Lower Cretaceous of Bernissart (Belgium). *Institut Royal des Sciences Naturelles de Belgique, Memoires 178*, 1–103

Otero, A., Krupandan, E., Pol, D., Chinsamy, A., & Choiniere, J. (2015). A new basal sauropodiform from South Africa and the phylogenetic relationships of basal sauropodomorphs. *Zoological Journal of the Linnean Society*, *174*(3), 589-634.

Plate, T., and Heiberger, R. (2016). abind: Combine Multidimensional Arrays. R package version 1.4-5. https://CRAN.R-project.org/package=abind

Pol, D., Garrido, A., & Cerda, I. A. (2011). A new sauropodomorph dinosaur from the Early Jurassic of Patagonia and the origin and evolution of the sauropod-type sacrum. *Plos One*, *6*(1), e14572.

R Core Team (2016). R: A language and environment for statistical computing. R Foundation for Statistical Computing, Vienna, Austria. URL https://www.R-project.org/.

Rauhut, O. W. (2006). A brachiosaurid sauropod from the late Jurassic Cañadón Calcáreo Formation of Chubut, Argentina. *Fossil Record*, *9*(2), 226-237.

Rauhut O.W., Fechner R.E., Remes K.R., Reis K.A. (2011). How to get big in the Mesozoic: the evolution of the sauropodomorph body plan. *Biology of the sauropod dinosaurs: Understanding the life of giants*.

Reisz, R. R., Scott, D., Sues, H. D., Evans, D. C., & Raath, M. A. (2005). Embryos of an Early Jurassic prosauropod dinosaur and their evolutionary significance. *Science*, *309*(5735), 761-764.

Reisz, R. R., Evans, D. C., Sues, H. D., & Scott, D. (2010). Embryonic skeletal anatomy of the sauropodomorph dinosaur *Massospondylus* from the Lower Jurassic of South Africa. *Journal of Vertebrate Paleontology*, *30*(6), 1653-1665.

Reisz, R. R., Evans, D. C., Roberts, E. M., Sues, H. D., & Yates, A. M. (2012). Oldest known dinosaurian nesting site and reproductive biology of the Early Jurassic sauropodomorph *Massospondylus*. *Proceedings of the National Academy of Sciences*, *109*(7), 2428-2433.

Remes, K. (2008). *Evolution of the Pectoral Girdle and Forelimb in Sauropodomorpha (Dinosauria, Saurischia): Osteology, Myology, and Function* (Doctoral dissertation, Ph. D. Dissertation. Ludwig-Maximilians-Universitat, Miinchen).

Remondino, F., Rizzi, A., Girardi, S., Petti, F. M., & Avanzini, M. (2010). 3D Ichnology—recovering digital 3D models of dinosaur footprints. *The Photogrammetric Record*, *25*(131), 266-282.

Rich, T. H., & Vickers-Rich, P. (2000). *Dinosaurs of darkness*. Indiana University Press.

Rose, M. D. (1989). New postcranial specimens of catarrhines from the Middle Miocene Chinji Formation, Pakistan: descriptions and a discussion of proximal humeral functional morphology in anthropoids. *Journal of Human Evolution*, *18*(2), 131-162.

Sander, P. M., Christian, A., Clauss, M., Fechner, R., Gee, C. T., Griebeler, E. M., & Preuschoft, H. (2011). Biology of the sauropod dinosaurs: the evolution of gigantism. *Biological Reviews*, *86*(1), 117-155.

Sander, P. M. (2013). An evolutionary cascade model for sauropod dinosaur gigantism-overview, update and tests. *PLoS One*, *8*(10), e78573.

Schlager, S. (2016). Morpho: Calculations and Visualisations Related to Geometric Morphometrics. R package version 2.4.1.1. https://CRAN.R-project.org/package=Morpho

Senter, P. (2006). Forelimb function in *Ornitholestes hermanni* Osborn (Dinosauria, Theropoda). *Palaeontology*, *49*(5), 1029-1034.

Senter, P. (2007). Analysis of forelimb function in basal ceratopsians. *Journal of Zoology*, *273*(3), 305-314.

Senter, P., & Robins, J. H. (2005). Range of motion in the forelimb of the theropod dinosaur *Acrocanthosaurus atokensis*, and implications for predatory behaviour. *Journal of Zoology*, *266*(3), 307-318.

Sereno, P. C., Forster, C. A., Rogers, R. R., & Monetta, A. M. (1993). Primitive dinosaur skeleton from Argentina and the early evolution of Dinosauria.

Sereno, P. C., & Novas, F. E. (1992). The complete skull and skeleton of an early dinosaur. *Science*, *258*(5085), 1137-1141.

Sertich, J. J., & Loewen, M. A. (2010). A new basal sauropodomorph dinosaur from the Lower Jurassic Navajo Sandstone of southern Utah. *PLoS One*, *5*(3), e9789.

Strang, K. T., & Steudel, K. (1990). Explaining the scaling of transport costs: the role of stride frequency and stride length. *Journal of Zoology*, *221*(3), 343-358.

Taylor, C. R., Heglund, N. C., & Maloiy, G. M. (1982). Energetics and mechanics of terrestrial locomotion. I. Metabolic energy consumption as a function of speed and body size in birds and mammals. *Journal of Experimental Biology*, *97*(1), 1-21.

Tschopp, E., Mateus, O., & Benson, R. B. (2015). A specimen-level phylogenetic analysis and taxonomic revision of Diplodocidae (Dinosauria, Sauropoda). *PeerJ*, *3*, e857.

Upchurch, P., Barrett, P. M., & Galton, P. M. (2007). A phylogenetic analysis of basal sauropodomorph relationships: implications for the origin of sauropod dinosaurs. *Special Papers in Palaeontology*, *77*, 57.

Upchurch, P., Mannion, P. D., & Taylor, M. P. (2015). The Anatomy and Phylogenetic Relationships of *Pelorosaurus "becklesii* (Neosauropoda, Macronaria) from the Early Cretaceous of England. *PLoS One*, *10*(6), e0125819.

VanBuren, C. S., & Bonnan, M. (2013). Forearm posture and mobility in quadrupedal dinosaurs. *PloS one*, *8*(9), e74842.

Wilson, J. A. (2005). Overview of sauropod phylogeny and evolution. *The sauropods: Evolution and paleobiology*, 15-49.

Wilson JA (2006) Anatomical nomenclature of fossil vertebrates: standardized terms or 'lingua franca'? *Journal of Vertebrate Paleontology 26*, 511-518

Yates, A. M. (2003). A definite prosauropod dinosaur from the lower Elliot Formation (Norian: Upper Triassic) of South Africa. *Palaeont. afr*, *39*, 63–68

Yates, A. M. (2004). *Anchisaurus polyzelus* Hitchcock: the smallest known sauropod dinosaur and the evolution of gigantism amongst sauropodomorph dinosaurs. Postilla 230, 1–58. 16. Galton PM and Upchurch P.(in press). Basal sauropodomorpha—prosauropods. *The Dinosauria*.

Yates, A. M. (2007). The first complete skull of the Triassic dinosaur *Melanorosaurus* Haughton (Sauropodomorpha: Anchisauria). *Evolution and palaeobiology of early sauropodomorph dinosaurs*, (77), 9-55.

Yates, A. M., & Kitching, J. W. (2003). The earliest known sauropod dinosaur and the first steps towards sauropod locomotion. *Proceedings of the Royal Society of London B: Biological Sciences*, *270*(1525), 1753-1758.

Yates, A. M., Bonnan, M. F., & Neveling, J. (2011). A new basal sauropodomorph dinosaur from the Early Jurassic of South Africa. *Journal of Vertebrate Paleontology*, *31*(3), 610-625.

Yates, A. M., Bonnan, M. F., Neveling, J., Chinsamy, A., & Blackbeard, M. G. (2010). A new transitional sauropodomorph dinosaur from the Early Jurassic of South Africa and the evolution of sauropod feeding and quadrupedalism. *Proceedings of the Royal Society of London B: Biological Sciences*, *277*(1682), 787-794.

Zelditch, M. L., Swiderski, D. L., & Sheets, H. D. (2012). *Geometric morphometrics for biologists: a primer*. Academic Press.

Zhao, Q., Benton, M. J., Sullivan, C., Sander, P. M., & Xu, X. (2013). Histology and postural change during the growth of the ceratopsian dinosaur *Psittacosaurus lujiatunensis*. *Nature communications*, *4*.